

# Advances in Quark Gluon Plasma

Ginés Martínez García

*SUBATECH, CNRS/IN2P3, École des Mines de Nantes,  
Université de Nantes, 4 rue Alfred Kastler, 44307 Nantes, France*

(Dated: April 5, 2013)

In the last 20 years, heavy-ion collisions have been a unique way to study the hadronic matter in the laboratory. Its phase diagram remains unknown, although many experimental and theoretical studies have been undertaken in the last decades. After the initial experiences accelerating heavy nuclei onto fixed targets at the AGS (BNL, USA) and the SPS (CERN, Switzerland), the *Relativistic Heavy Ion Collider* (RHIC) at BNL was the first ever built heavy-ion collider. RHIC delivered its first collisions in June 2000 boosting the heavy-ion community. Impressive amount of experimental results has been obtained by the four major experiments at RHIC: PHENIX, STAR, PHOBOS and BRAHMS. In November 2010, the *Large Hadron Collider* (LHC) at CERN delivered lead-lead collisions at unprecedented center-of-mass energies, 14 times larger than that at RHIC. The three major experiments, ALICE, ATLAS and CMS, have already obtained many intriguing results. Needless to say that the heavy-ion programs at RHIC and LHC promise fascinating and exciting results in the next decade.

The first part of the lectures will be devoted to introduce briefly the QCD description of the strong interaction (as part of the Standard Model of Particle Physics) and to remind some basic concepts on phase transitions and on the phase diagram of matter.

In the second part, I will focus on the properties of matter at energy densities above  $\approx 1 \text{ GeV/fm}^3$ . A historical approach will be adopted, starting with the notion of limiting temperature of matter introduced by Hagedorn in the 60's and the discovery of the QCD asymptotic freedom in the 70's. The role played by the chiral symmetry breaking and restoration in the QCD phase transition will be discussed, supported by an analogy with the ferromagnetic transition. The phase diagram of hadronic matter, conceived as nowadays, will be shown together with the most important predictions of lattice QCD calculations at finite temperature. Finally, the properties of an *academic* non-interacting ultra-relativistic QGP and its thermal radiation will be deduced. The dissociation of the heavy quarkonium due to the color-screening of the heavy-quark potential will be described, based on a QED analogy. The energy-loss phenomenology of ideal long-living partons traversing the QGP, will be reminded.

In the third part, the heavy-ion collisions at ultra-relativistic energies will be proposed as a unique experimental method to study QGP in the laboratory, as suggested by the Bjorken model. The main experimental facilities in the world will be described, namely the CERN and BNL accelerator complexes. The main probes for characterizing the QGP in heavy-ion experiments, followed by a brief description of the main heavy-ion experiments located at these facilities will be shown.

In the last part of these lectures, I will present my *biased* review of the numerous experimental results obtained in the last decade at RHIC which lead to the concept of strong interacting QGP, and the first results obtained at LHC with the 2010 and 2011 PbPb runs. Finally, the last section is devoted to refer to other lectures about quark gluon plasma and heavy ion physics.

## CONTENTS

I. Introduction	3
A. Asymptotic freedom	3
B. Lattice QCD calculations	4
C. A description of the hadronic matter phase diagram	5
II. The Quark Gluon Plasma	6
A. Limiting temperature of matter	6
B. Deconfined state of matter	7
C. The spontaneous break-up of chiral symmetry in QCD	8
D. Some results from lattice QCD calculations at finite temperature	10
E. Properties of a QGP in the ultra-relativistic limit	12
F. Probes of the QGP	14
1. Thermal radiation	14
2. Screening of the colour potential between heavy quarks in the QGP	15
3. Parton - QGP interaction	17
III. Heavy Ion Collisions and Heavy Ion Accelerators	18
A. The Bjorken scenario of heavy ion collisions at ultra-relativistic energies	19
1. Formation.	21
2. Thermalisation.	21
3. Longitudinal expansion.	22
4. 3D expansion and freeze-out phase.	22
B. Heavy ion accelerators and colliders	22
1. The Alternating Gradient Synchrotron at BNL	23
2. The Super Proton Synchrotron at CERN	23
3. The Relativistic Heavy Ion Collider at BNL	24
4. The Large Hadron Collider at CERN	24
IV. Some bases about collision centrality and the nuclear modification factor	25
V. Brief summary of the experimental results at RHIC and at the LHC	25
A. Initial energy density	25
B. Equilibration	26
C. Initial temperature	29
D. The phase of deconfinement	31
E. The opacity of the QGP	32
F. Other interesting measurements	34
G. Caveat on cold nuclear matter effects	35
VI. Other lectures on QGP	35
VII. Acknowledgements	36
References	36

## I. INTRODUCTION

The strong interaction, described by quantum chromodynamics (QCD), is the dominant interaction in the subatomic world. The main properties of the strong interaction are:

- the strength constant  $\alpha_s$  at low energies is large, and as a consequence, quantitative calculations based on a perturbative sum of Feynman diagrams, fail<sup>1</sup>;
- gluons,  $g$  (the intermediate boson of strong interaction) are coloured (colour is the charge of the strong interaction). For this reason, the QCD becomes a complex quantum field theory (QFT), which belongs to the class of non-abelian QFT.

The quarks  $u$ ,  $d$  and  $s$ , also called light quarks, exhibit small masses and therefore the most important parameter of QCD is indeed  $\alpha_s$ . However  $\alpha_s$  can only be determined in the high energy domain, since its experimental determination at low energy is difficult due to non-perturbative effects. One of the major experimental observations that QCD should explain, is the confinement of quarks and gluons. Coloured free particles do not exist, and thus quarks and gluons seem to be confined inside colourless particles called hadrons. The confinement property is not fully understood, despite the fact that the quark model describes qualitatively the hadron properties (mesons are bound states of a quark and antiquark and baryons are bound states of 3 quarks). Today, the best *ab-initio* quantitative calculations can be performed via lattice calculations of QCD. One should note that the origin of the hadron mass is the strong interaction, since light quark masses only represent less than 10% of the total hadron mass. As Frank Wilczek (Nobel prize in 2004) expressed in Physics Today in November 1999 *"According to quantum chromo-dynamics field theory, it is precisely its color field energy that mostly make us weigh. It thus provides, quite literally, mass without mass"*. In this respect the Higgs boson (strictly speaking the Brout-Englert-Higgs boson or BEH boson) only explains about 1% of the total mass of the proton and neutron which are the main massive constituents of ordinary matter.

### A. Asymptotic freedom

The vacuum polarization of QCD [Politzer 73, Gross 73] exhibits a singular behaviour due to the anti-screening effect of virtual gluon pair production (remember that gluons are colored bosons and the gluon vertex does exist in QCD). Indeed the gluon anti-screening is stronger than the screening effect of virtual quark pair production (see Fig. 1). In QCD one gets [Griffiths 87]:

$$\alpha(|q^2|) = \frac{\alpha_s(\mu^2)}{1 + \frac{\alpha_s(\mu^2)}{12\pi}(11n - 2f) \ln(|q^2|/\mu^2)} \quad (1)$$

where  $n$  represent the number of colors and  $f$  the number of quark flavors. In nature,  $11n > 2f$ , in consequence, the strength of the strong interaction  $\alpha_s$  decreases at small distances (or high energies). This phenomenon is called the *asymptotic freedom* of QCD. The discovery of the asymptotic freedom was awarded with the Nobel Prize in 2004<sup>2</sup>.

At the scale of the Z boson mass ( $|q^2| \sim M_Z$ ),  $\alpha_s$  has been measured via many different physics channels and the current world average is  $0.1184 \pm 0.0007$  [Beringer 12]. Perturbative QCD calculations are then fully valid to describe the strong interaction at high energies. This is one of the major successes of QCD theory.

<sup>1</sup> Roughly, the strength constant  $\alpha_s$  can be estimated from the hadron bound state properties. Using the Bohr radius expression of the hydrogen atom (please forgive me this unacceptable assumption)  $r_B = 2/(m\alpha)$ , one can estimate  $\alpha_s \sim 20$ , considering  $r_B = 1$  fm and  $m_q = 10$  MeV.

<sup>2</sup> [http://www.nobelprize.org/nobel\\_prizes/physics/laureates/2004/](http://www.nobelprize.org/nobel_prizes/physics/laureates/2004/)

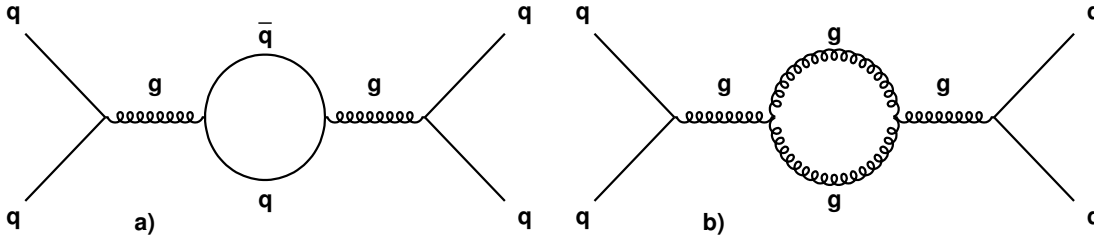


FIG. 1. *Feynman diagrams at first order, of the vacuum polarization in QCD: a) screening and b) anti-screening. In the case of QED, anti-screening does not exist since photons are not charged particles.*

In equation (1), the parameter  $\mu^2$  is imperative since perturbative QCD calculations cannot be performed in the domain where  $\alpha_s \gtrsim 1$  (when  $|q^2| \lesssim 1 \text{ GeV}^2$ ). The expression (1) can be rewritten as a function of a parameter  $\Lambda_{QCD}$ :

$$\alpha(|q^2|) = \frac{12\pi}{(11n - 2f) \ln(|q^2|/\Lambda_{QCD}^2)}. \quad (2)$$

$\Lambda_{QCD}$  is  $213 \pm 8 \text{ MeV}$  for 5 flavours [Beringer 12]. However, the quantity  $\Lambda_{QCD}$  is not well defined. Therefore it has become standard practice to quote the value of  $\alpha_s$  at a given scale (typically  $M_Z$ ) rather than to quote a value for  $\Lambda_{QCD}$  [Beringer 12].

## B. Lattice QCD calculations

As we have previously seen, the asymptotic freedom is the main success of QCD and it allows for the experimental test of QCD via the study of high energy processes. I would say that the description of i) the evolution of the parton distribution functions at low Bjorken  $x$  values, ii) the production of jets in elementary collisions and iii) the properties of bottomonium bound states, represent beautiful examples of the success of QCD predictions in its perturbative domain.

Nevertheless QCD should a priori explain many other phenomena where perturbative calculations are forbidden. Fundamental questions such as the coupling constant value, QCD vacuum structure, hadron masses, hadron structure, nuclear properties etc ... should be explained by the QCD theory. Even today, the test of QCD has not been possible in many of these domains. In order to palliate this, many effective models have been developed in the domain of hadronic and nuclear physics.

Lattice calculation for gauge theories is the most promising non-perturbative technique to solve QCD equations. The space-time continuum is discretized in a finite number of points where the equations of the theory can be solved. In the last decade, the impressive development of computing hardware and the optimization of software algorithms have allowed lattice QCD calculations to become a competitive tool [Wilczek 03]. Nowadays computing facilities for lattice QCD calculations are a crucial component of this research, at the same level as accelerators, detectors or computing centers for data analysis and data storage. Today lattice QCD provides the most precise computation of the  $\alpha_s$  constant, is able to extract the mass of the quarks and to predict the mass of most of the hadrons, and it makes excellent predictions of the exotic structure of new bound states of heavy quarks. In particular, we will see later in more detail, how lattice QCD at finite temperature allows to study the hadronic matter phase diagram.

### C. A description of the hadronic matter phase diagram

By hadronic matter I mean that in which the strong interaction is the main interaction between elementary constituents, that provide the proper degrees of freedom of the matter. At temperatures above  $10^9$  K (1 MeV) and/or pressures above  $10^{32}$  Pa (1 MeV/fm<sup>3</sup>), the strong interaction is expected to be the dominant interaction between the constituents of matter. At low temperatures and a pressure above 1 MeV/fm<sup>3</sup> the matter can be described as a degenerated gas of neutrons<sup>3</sup>. Such a state, which is very close to the atomic nucleus structure, should exist in the neutron stars. In these stellar objects, a mass slightly larger than the sun mass, is confined in a ten kilometer radius sphere, and densities as high as  $10^{17}$  kg/m<sup>3</sup> are reached. For higher pressures, above  $10^{35}$  Pa (1 GeV/fm<sup>3</sup>), the repulsive force of the degenerate gas of neutrons cannot compensate the pressure, and matter is expected to become a low temperature gas of quarks which are not any more confined inside hadrons. In this exotic state of matter, quark-quark Cooper pairs might exist creating a kind of color superconductor matter [Rajagopal 00]. On the other hand, the neutron matter should become a gas of nucleons, if it is heated to temperatures of several MeV. Indeed the nucleon-nucleon potential has some similitudes with the Van der Waals force between molecules. For this reason, it is expected that the neutron matter evaporates into a gas of nucleons at a temperature of about 10 MeV<sup>4</sup>, like the liquid-gas phase transition in ordinary matter.

At very high temperatures and pressures, the nucleon gas (that has become a hadron gas at temperature above 100 MeV) could go through a transition to a deconfined state of matter. This is expected due to the vacuum polarization at the origin of the asymptotic freedom of QCD. Therefore the strength of the strong force decreases at high temperature. The deconfined state of matter, in analogy with the electromagnetic plasma where ions and electrons are dissociated, has been called Quark Gluon Plasma (QGP)<sup>5</sup>. The transition to QGP takes place at temperatures about 200 MeV ( $\sim 2 \cdot 10^{12}$  K), when quarks and gluons are not confined in colorless particles and they become the pertinent degrees of freedom of the system. Other properties of QCD also predict the reason that a phase transition should occur at high temperature. In quantum field theories, the symmetries of the Lagrangian can be spontaneously broken at low energies or temperatures. In the case of QCD, the spontaneous breaking of the chiral symmetry takes place at low temperature. The restoration of the chiral symmetry at high temperatures becomes a sufficient condition for the existence of a phase transition [Smilga 03].

Finally, for temperatures above  $10^{16}$  K, it is hard to know what would be the structure of matter. Some authors have speculated about new phenomena like formation of microscopic black holes or unification of interactions, etc ... that could appear. Exotic ideas like the formation of a superstring gas have been proposed for temperatures of  $10^{32}$  K [Bowick 85].

In Fig. 2, the lay-out of the phase diagram of matter is presented. We clearly distinguish two regions, one for temperatures below  $10^9$  K and pressures below  $10^{30}$  Pa, where the electromagnetic interaction between atoms (or ions) provides the degrees of freedom of matter, and a second region, for temperatures above  $10^9$  K and/or pressures above  $10^{32}$  Pa, where the strong interaction between nucleons, hadrons or quarks dominates and provides the right degrees of freedom.

<sup>3</sup> Actually, it is a degenerate gas of baryons and electrons which is a more stable system than a pure neutron gas.

<sup>4</sup> Naively, this value can be accepted since the bound energy of nucleus in the nuclei saturates to a value of 8 MeV. The liquid-gas transition has been studied in heavy ion collisions at intermediate energies, although it is not discussed in these lectures.

<sup>5</sup> Professor E. Shuryak proposed the name Quark Gluon Plasma in the 80's [Shuryak 78].

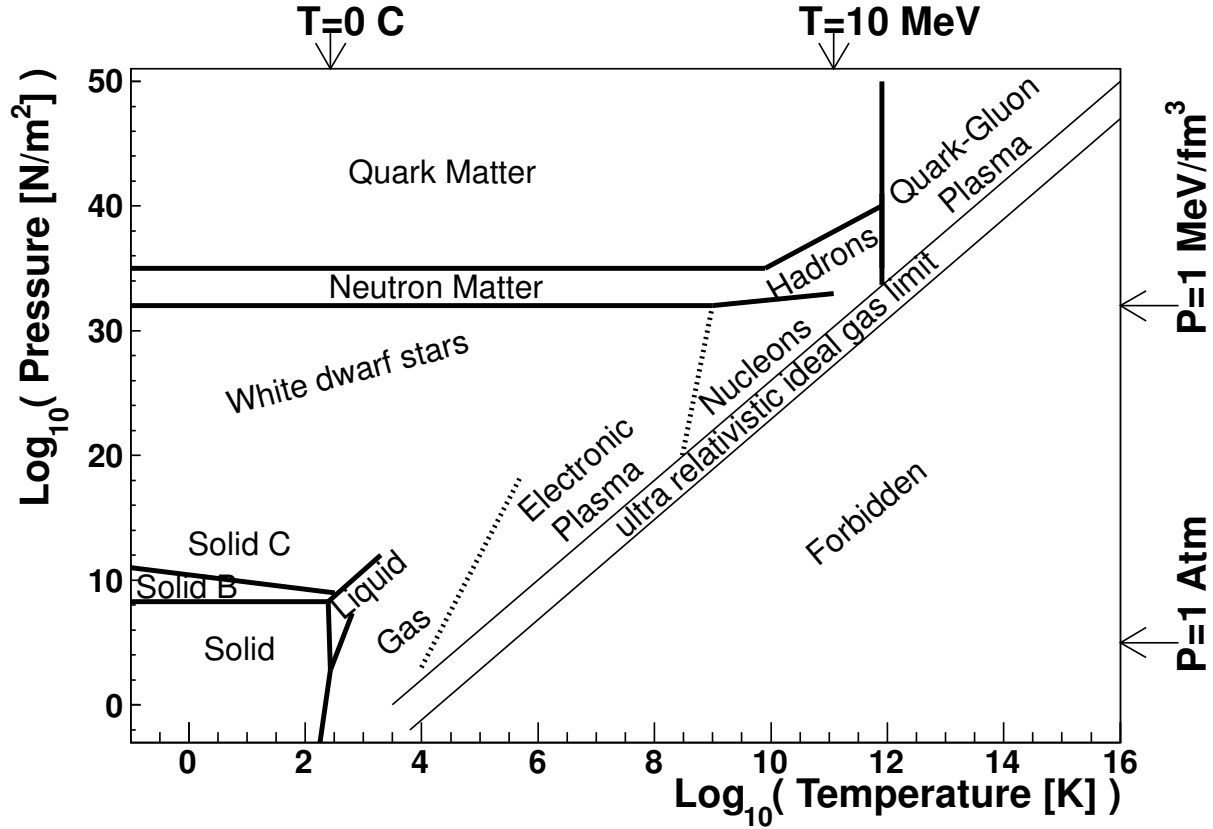


FIG. 2. Phase diagram of matter in the pressure versus temperature plane for a non zero baryonic potential [Martínez 06].

## II. THE QUARK GLUON PLASMA

### A. Limiting temperature of matter

Curiously, the first prediction of a critical behaviour of hadronic matter at high temperature was obtained before the formulation of QCD and the discovery of partons [Hagedorn 65, Hagedorn 84]. At mid 60's, Hagedorn was interested in properties of the hadron gas. He predicted in a phenomenological and original manner, that should exist a critical behaviour of the hadron gas at high temperature [Hagedorn 65]. Hagedorn interpreted this criticality as the existence of a maximum temperature of matter, that was called Hagedorn's temperature  $T_H$ . In order to study the hadron gas, one has to consider all the *zoology* of hadron particles. Today, more than 2000 hadron species have been discovered (see Fig. 3 left). Hagedorn studied the number of hadron species as a function of their mass. He observed an exponential dependence and the following function was used to describe the experimental data:

$$\rho(m) = \frac{A}{m^2 + [500\text{MeV}^2]} \exp(m/T_H) \quad (3)$$

where  $\rho(m)$  is the density of hadron species per mass unit and  $T_H$  is a parameter. From the experimental data, one obtains that the parameter  $T_H$  is close to the mass of the pion,  $\sim 180\text{ MeV}$ , when all the known baryon and meson resonances are considered [Broniowski 04]. It turns out that such a dependence of the density  $\rho(m)$  will induce divergences of the partition

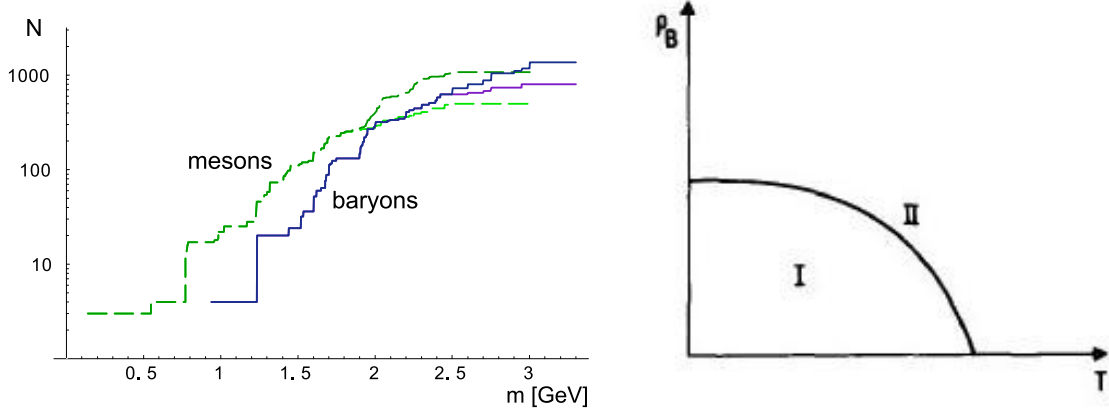


FIG. 3. *Left: number of hadron species as a function of their mass [Broniowski 04]. Right: first phase diagram of hadronic matter [Cabibbo 75].  $\rho_B$  is the baryonic density,  $T$  the temperature, (I) is the confined phase and (II) is the deconfined phase.*

function that describes the statistical properties of a hadron gas, if the temperature of matter reaches values above the Hagedorn parameter  $T_H$ . In consequence,  $T_H$  was interpreted as a limiting temperature of matter. Somehow, any additional energy supplied to the system at the Hagedorn temperature, would be used to create new hadron species.

We know that hadrons are not point-like particles, and their typical size is around 1 fm sphere radius. Indeed, when one gets closer to the  $T_H$  temperature, the hadron density increases (remember that the energy density of an ideal ultra-relativistic gas increase as  $T^4$ ) and values about 1 hadron per  $\text{fm}^3$  are reached. Under these conditions, hadrons overlap with each other and considering hadrons as point-like particles (which means that their size is small with respect to its mean free path) becomes a wrong hypothesis and invalidate Hagedorn conclusions. Therefore one has to understand first the internal structure of hadrons, since it is going to provide the new degree of freedom of the system when  $T \geq T_H$ . Only QCD was able to answer this question several years later.

## B. Deconfined state of matter

After the discovery of the asymptotic freedom [Politzer 73, Gross 73], the existence of a deconfined state of quarks and gluons was predicted at high temperature and/or high pressures [Collins 75, Cabibbo 75]. A first pioneer phase diagram of hadronic matter was imagined (see Fig. 3 right from reference [Cabibbo 75]). At sufficiently high temperatures, quarks and gluons interact weakly and the system will behave as an ideal ultra-relativistic gas. The degrees of freedom will be then determined by the flavor numbers, spin states, color and charge states of the quarks and gluons. The deconfined state was called later quark gluon plasma [Shuryak 78]. The word *plasma* is used to describe the state of matter when ions and electrons are dissociated in atoms. There is then an analogy when colourless particle dissociate to create deconfined matter. One open question after the discovery of the asymptotic freedom, concerned the properties of the transition from the hadron gas to the QGP: does it take place smoothly or via a phase transition and exhibiting critical behaviours? As a matter of fact, the transition from gas to electronic plasma takes place smoothly in the temperature range 10000 to 50000 K [Stocker 99] and no critical behaviour is therefore observed. The question whether the QGP phase transition exists, is, of course, a very deep question and the intrinsic symmetries of the QCD could give us the answer. Indeed the chiral symmetry of the massless quark QCD Lagrangian is spontaneously broken

at low temperature and this symmetry should be restored at high temperatures. A symmetry restoration represents a valid condition to predict the existence of a QCD phase transition. It remained however an open question if the chiral symmetry transition and the deconfinement transition are or not the same one. Only lattice calculations have been able to provide an answer to this question as we will see later.

### C. The spontaneous break-up of chiral symmetry in QCD

A simplified Lagrangian of 3 quark flavours  $f$  ( $u, d, s$ ) can be written as [Schaefer 05]:

$$\mathcal{L} = \sum_f^{N_f} \bar{\psi}_f (i\not{D} - m_f) \psi_f - \frac{1}{4} G_{\mu\nu}^a G_{\mu\nu}^a, \quad (4)$$

where  $N_f = 3$  and the coupling gluon field tensor is defined as:

$$G_{\mu\nu}^a = \partial_\mu A_\nu^a - \partial_\nu A_\mu^a + g f^{abc} A_\mu^b A_\nu^c, \quad (5)$$

and the covariant derivate of the quark field as:

$$i\not{D}\psi = \gamma^\mu \left( i\partial_\mu + g A_\mu^a \frac{\lambda^a}{2} \right) \psi. \quad (6)$$

Under these conditions, the previous Lagrangian exhibits a flavour symmetry since the quark interaction does not depend on the quark flavour. This is indeed always the case if the masses of the quarks are identical. The direct consequence of this is the symmetry under isospin transformations, that it is observed in the hadron properties. In addition, for massless quarks, the QCD Lagrangian exhibits the chiral symmetry<sup>6</sup>. The quark fields can be decomposed in left-hand and right-hand quarks fields [Halzen 84]:

$$\psi_{L,R} = \frac{1}{2}(1 \pm \gamma_5)\psi. \quad (7)$$

As a consequence, the QCD Lagrangian is invariant under helicity and flavour transformations. This symmetry is represented as the  $SU(3)_L \times SU(3)_R$  symmetry of QCD. One of the consequences of this symmetry is that the associated parameter, called *condensate*  $\langle q\bar{q} \rangle$  should be zero.

Nevertheless, the *condensate*  $\langle q\bar{q} \rangle$  is not zero and the existence of the pion is a clear confirmation of this statement [Knecht 98]. This is what it is called the *spontaneous* breaking of the  $SU(3)_L \times SU(3)_R$  chiral symmetry of QCD. The word *spontaneous* reminds us that the symmetry is respected by the QCD Lagrangian but broken by their states at low energies. At high energies the symmetry should be restored.

The spontaneous breaking of a symmetry is a phenomenon that is allowed in quantum field theories, where the structure of the vacuum plays a major role. In quantum mechanics, the eigenstates that respect the symmetry of the Hamiltonian, can always be found. In classical mechanics the following analogy of the spontaneous symmetry breaking can be found. Let's assume a ring in the earth gravitational field, that rotates along its vertical symmetry axis with an angular speed  $\omega$ . There is a small solid ball with a hole in a manner that can move freely along the ring (see Fig. 4). In this example, the system exhibits a left-right symmetry which is spontaneously broken by the small ball at low internal energy.

---

<sup>6</sup> Chiral from *hand* in Greek.



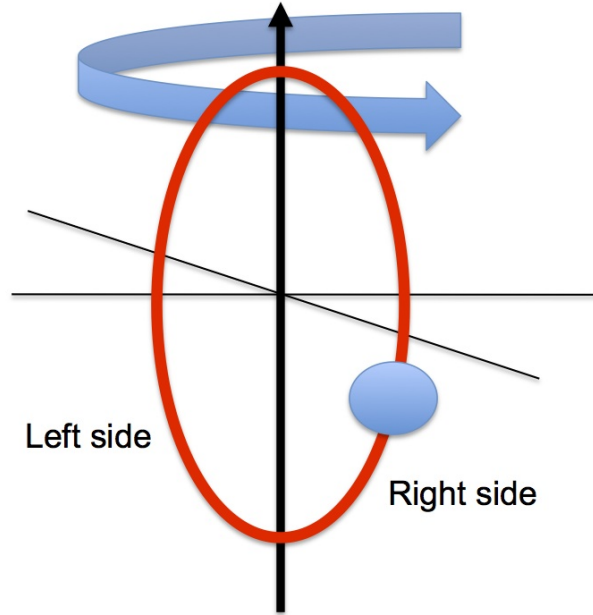


FIG. 4. *Classical analogy of spontaneous symmetry breaking. The ball is holed and can move freely along the ring, which rotates with an angular speed  $w$ , in the earth gravitational field with respect to its vertical symmetry axis.*

Indeed, due to the centrifugal force, the small ball has to choose the left or the right side of the ring as its equilibrium position. If some internal energy is given to the ball, it will start to oscillate around its equilibrium position. The amplitude of the oscillation will increase with the internal energy of the ball. Above a certain energy threshold, the ball will have enough internal energy to reach the other side of the ring and it will then move in both sides. When this occurs, one can say that the left-right symmetry of the system has been restored.

The spontaneous breaking of the chiral symmetry is one of the predictions of QCD [Knecht 98], and, in this way, QCD is able to predict the existence of the Goldstone bosons: the pions, kaons and eta mesons and to explain their small interaction cross-sections. As in the classical analogy, the chiral symmetry of the QCD is restored at high energies (or high temperatures) and remember that a restoration of the symmetry represents a sufficient condition for the existence of a QCD phase transition. An analogy with the ferromagnetic phase transition can be made (see table I) [Schaefer 05]. In fact, the ferromagnetic phase transition can be associated to the spontaneous breaking of the isotropy symmetry. At high energy the ferromagnetic system is invariant under rotation transformation, since there is not any privileged direction of the space. Nevertheless at low temperatures, the thermal agitation cannot avoid that the microscopic magnetic moments of the elementary constituents align, causing a macroscopic magnetisation of the system. Therefore the isotropy symmetry is spontaneously broken at low temperatures, and this is a sufficient condition to predict that there is a phase transition during the generation of the macroscopic magnetisation of the system. In the ferromagnetic case, the magnetisation  $\vec{M}$  is the order parameter of the transition, which is the equivalent of the quark condensate  $\langle q\bar{q} \rangle$  in the chiral transition in QCD. The non-zero  $\vec{M}$ , allows for the existence of spin waves, and the Goldstone bosons (pions, kaons and eta's) are their analogues. Finally, isotropy symmetry can be explicitly

Transition	Chiral	Ferromagnetic
Spontaneous breaking	$SU(3)_L \times SU(3)_R$	Isotropy $O(4)$
Order parameter	Condensate $\langle q\bar{q} \rangle$	Magnetisation $\vec{M}$
States	Goldstone bosons $\pi, K, \dots$	Spin waves
Explicit breaking	Quark masses $m_q \neq 0$	External magnetic field

TABLE I. Analogy between the chiral and the ferromagnetic phase transition [Schaefer 05].

broken via an external magnetic field. The equivalent of the non-zero external magnetic field would be the non-zero masses of the quarks, which explicitly breaks the chiral symmetry of the QCD Lagrangian.

We have seen that a spontaneous breaking of the chiral symmetry explains why there should be a phase transition of the hadronic matter. We can now wonder if such a transition is associated to the process of deconfinement of quarks and gluons leading to the formation of a quark gluon plasma. One could imagine that there are, indeed, two different phase transitions, a chiral transition and a deconfinement one that occur at different critical temperatures. In the next section, lattice QCD calculations will be presented since this is the only way to answer this question today.

It should be noted that we have assumed a QCD Lagrangian with massless  $u$ ,  $d$  and  $s$  quarks. This is indeed a good approximation, since the masses of the, so called light quarks, are small compared to  $\Lambda_{QCD}$  but they are not zero:  $m_u = 2.3 \pm 0.5$  MeV,  $m_d = 4.8^{+0.7}_{-0.3}$  MeV and  $m_s = 95 \pm 5$  MeV [Beringer 12]. In this respect the chiral symmetry is indeed explicitly broken by the QCD Lagrangian. Above we have assumed that if the masses are small compared to  $\Lambda_{QCD}$  this chiral symmetry should remain a good symmetry of QCD. However this may be a wrong assumption, in particular for the strange quark. Indeed, it is an open question what would be the masses value thresholds causing the damp out of the criticalness of the chiral transition. Above such mass thresholds, the chiral transition would become a cross-over and no critical behaviour would be observed in the transition. Once more, the lattice QCD calculations will be a unique method to study this question.

Finally, there is a new symmetry of the QCD Lagrangian in the limit of quarks masses  $m_q \rightarrow \infty$ . The order parameter of this symmetry is called the Polyakov line  $\langle P \rangle$  which is directly associated to the process of deconfinement if  $\langle P \rangle = 0$  [Schaefer 05].

#### D. Some results from lattice QCD calculations at finite temperature

Today, lattice QCD calculation is a unique method to test QCD in the non-perturbative domain. In the last decades, many progresses have been achieved on the algorithms and on the computing performances. Lattice QCD allows for non-perturbative calculations with high reliability.

In particular, lattice QCD should allow to study the properties of the Universe between few ns and few  $\mu s$  after the Big Bang (temperatures around 100-1000 MeV) and to study hadronic matter in the core of the neutron stars [Petreczky 12]. For massless quarks, these calculations show a transition at baryonic potential  $\mu_B = 0$ , as expected from the spontaneous breaking of the chiral symmetry in QCD. The critical temperature would be  $T = 173 \pm 15$  MeV and the critical energy density  $\epsilon = 0.7 \pm 0.3$  GeV/fm<sup>3</sup> [Karsch 02a] (see Fig. 5). It is also observed that above the critical temperature, the energy density is indeed proportional to  $T^4$ , as for an ideal ultra-relativistic gas, but the proportionality factor (Stefan-Boltzmann constant) is about 20% smaller than the expected value for an ideal gas of gluons and massless  $u$ ,  $d$  and  $s$  quarks. Perturbative calculations at higher temperatures

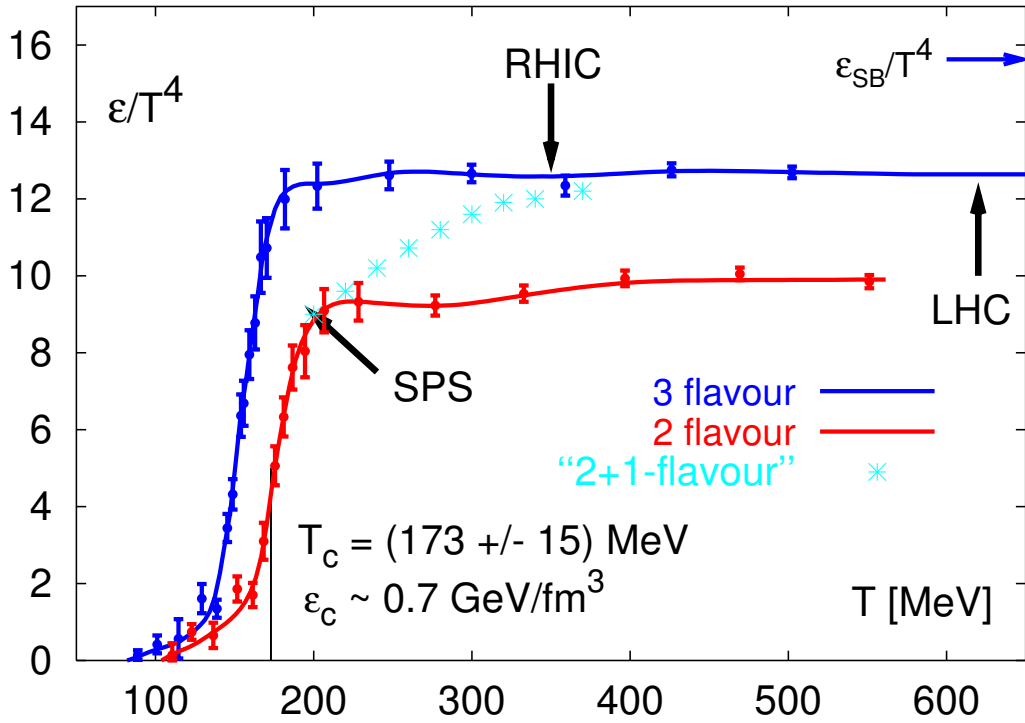


FIG. 5. Dependence of the energy density as a function of the temperature of the hadronic matter at null baryonic potential given by lattice QCD calculations at finite temperature. The calculations are performed for two massless quarks, three massless quarks and two massless quark and one ( $s$ ) with its real mass. A transition is observed at a temperature of about 173 MeV and energy density of 0.7 GeV/fm<sup>3</sup>. For the calculations with a real  $s$  mass, the transition is faded away [Karsch 02a]

are able to explain the evolution of this factor for  $T \geq 2T_c$  [Blaizot 99].

The lattice QCD calculations show that for massive quarks, the phase transition could fade away, it would become a cross-over and no criticalness would be observed. The criticalness of the transition has been studied as a function of the quark masses (see Fig. 6). In the calculations presented here, the  $u$  and  $d$  masses are considered to be identical and  $\mu_B = 0$ . It is observed that for both low and large masses, a 1st order phase transition is predicted. The cross-over transition occurs for intermediate quark masses. A 2nd order phase transition occurs in the border line between 1st order and cross-over areas. Today there is some consensus to believe that for the physical quark masses and  $\mu_B = 0$  there is not a phase transition but a cross-over [Karsch 02a, Karsch 02b]<sup>7</sup>.

The QCD lattice calculations with physical quark masses, have determined critical temperatures between 150-200 MeV. There has been some confusion about the exact critical temperature of the transition in the last years. The outcome was that the evaluation of the transition temperature, which is not a well defined parameter for a cross-over transition, would depend on the method used for its determination. Calculations based on chiral order parameter show a cross-over transition for  $T \sim 155$  MeV. On the other hand, the behaviour of the Polyakov loop suggests that colour screening sets in at temperatures that are higher than the chiral transition temperature [Petreczky 12].

Finally, lattice QCD calculations have studied the order parameters of the chiral and deconfinement transitions (see Fig. 7) showing that, a priori, both transitions occur at the

<sup>7</sup> Note that more recent references on this subject exist and they are not referenced in this lecture.

### 3-flavour phase diagram

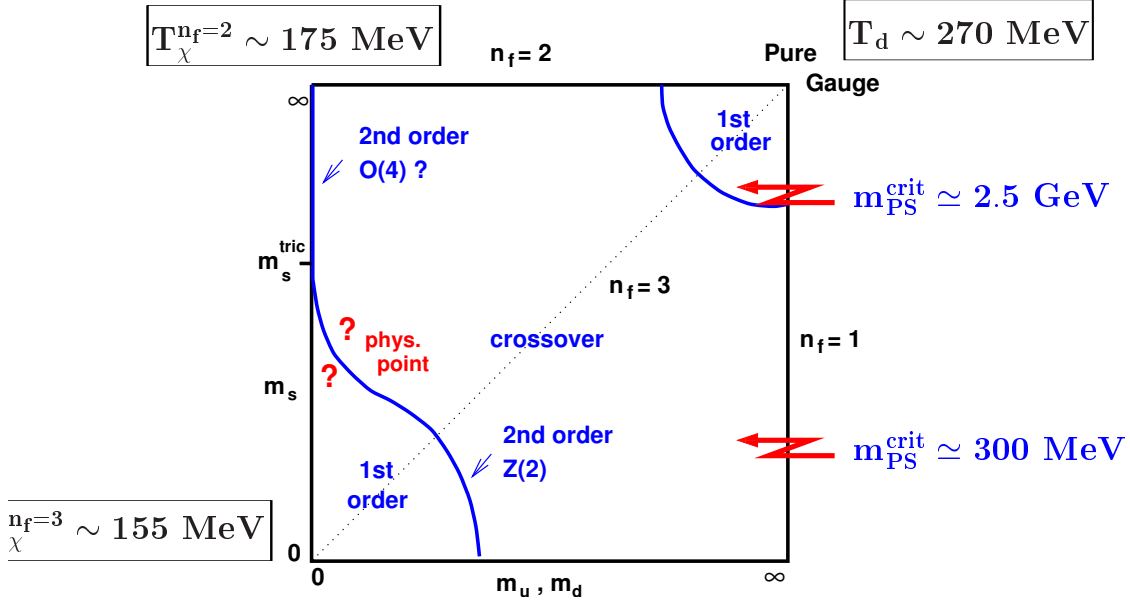


FIG. 6. Lattice QCD calculations of the criticalness of the hadronic matter phase transition for 3 quark flavours,  $\mu_B = 0$  and assuming the mass of the  $u$  and  $d$  quarks are identical and a strange quark mass,  $m_s$  [Karsch 02b, Karsch 02a].

same critical temperature. Therefore, this suggests that both transitions would be indeed the same transition. However, the interplay between chiral and deconfinement aspects of the transition appears to be more complicated than earlier lattice studies suggested. It seems that there is no transition temperature that can be associated with the deconfining aspects of the transition for physical values of the light quark masses [Petreczky 12].

In the last decade, a lot of effort has been done to perform calculations at  $\mu_B \neq 0$ . These calculations show that there would be a critical point at  $\mu_B \sim 0.75M_N$  ( $M_N$  is the nucleon mass) where the cross-over becomes a 2nd order phase transition, and beyond it, the transition becomes a 1st order phase transition between the gas of hadrons and the quark gluon plasma [Fodor 03]. In addition, other calculations have predicted a transition to a colour superconductor matter at high values of  $\mu_B$  (see the lay-out of the hadronic matter phase diagram in Fig. 8).

#### E. Properties of a QGP in the ultra-relativistic limit

At temperatures  $\Lambda_{QCD} \leq T \leq$  charm mass,  $m_c$  and assuming that the strong interaction strength becomes very small, the QGP would behave as an ideal gas. Strictly speaking this gas will be constituted by all the elementary particles ( $m \lesssim T$ ): leptons (electrons and muons), bosons (photons and gluons) and light quarks  $u$ ,  $d$  and  $s$ <sup>8</sup> and their corresponding antiparticles. This gas will have similar properties as the black body radiation and the equation of state is given by  $\epsilon = 3p$ , where  $\epsilon$  is the energy density and  $p$  is the pressure. The energy density will depend on the temperature following the Stefan-Boltzmann law  $\propto T^4$ .

<sup>8</sup> We assume a temperature lower than the mass of the charm quark and in this manner one could neglect the thermal production of heavy quarks, tau leptons and weak bosons

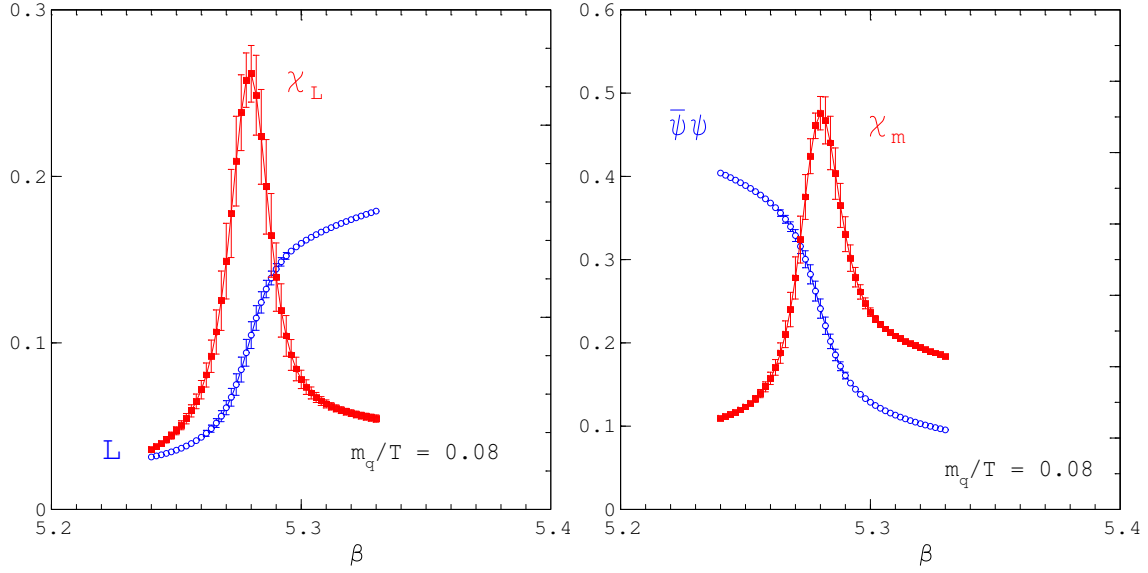


FIG. 7. Critical behaviour for massless quarks and  $\mu_B = 0$  of the order parameters of the deconfinement (left plot) and of the chiral (right plot) transitions as predicted by lattice QCD calculations. The order parameters are the Polyakov susceptibility ( $\chi_L$ ) and the chiral susceptibility ( $\chi_m$ ) [Karsch 02a]. Both transitions would indeed be the same one or would take place at the same critical temperature.

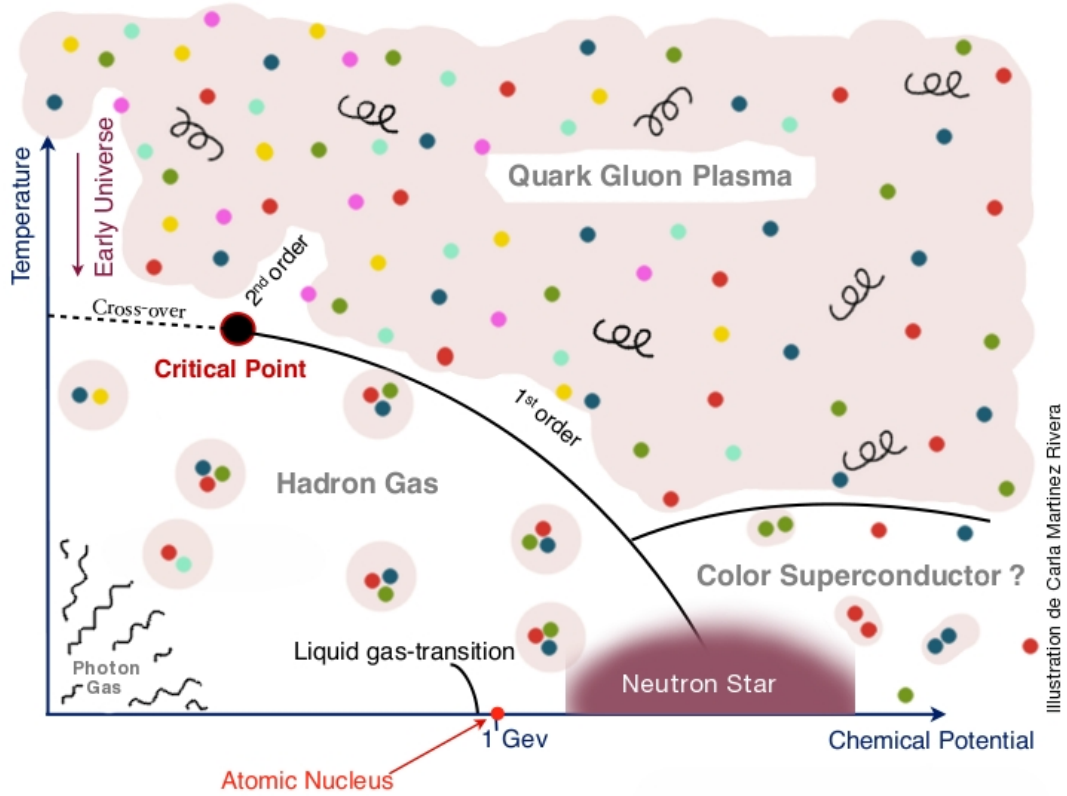


FIG. 8. Lay-out of the hadronic matter phase diagram as it is today conceived.

The Stefan-Boltzmann law for bosons is [Landau 67, Greiner 95]:

$$\epsilon_b = 3p = g \frac{\pi^2}{(\hbar c)^3} \frac{(k_B T)^4}{30} \quad (8)$$

where  $g$  is the number of degrees of freedom due to spin, flavour, and colour charge of the considered particle. In consequence,  $\epsilon/T^4$  or  $p/T^4$  will be constant for such a matter. If one only considers photons (black body radiation) we obtain the Stefan-Boltzmann constant ( $g=2$  for the two possible spins of the photon):

$$\sigma = \frac{\pi^2 k_B^4}{60 \hbar^3 c^2} = 5.670 \cdot 10^{-8} \text{ Wm}^{-2} \text{K}^{-4}. \quad (9)$$

In natural units (temperature in MeV), the equation of a photon gas is

$$\epsilon_\gamma = A \times T^4 [\text{MeV}^4] \quad (10)$$

with  $A \sim 0.65$ . The Stefan-Boltzmann law for fermions is similar to that for bosons [Landau 67, Greiner 95]:

$$\epsilon_f = 3p = g \frac{7\pi^2}{(\hbar c)^3} \frac{(k_B T)^4}{240}. \quad (11)$$

The total energy density of this matter will be:  $\epsilon = \epsilon_\gamma + \epsilon_l + \epsilon_g + \epsilon_q$ ; with  $g = 8$  for leptons (2 for spin, 2 for flavors and 2 particle-antiparticle),  $g = 16$  for gluons (2 helicity states and 8 colour charges) and  $g = 36$  for quarks (2 for spin, 3 colours, 3 flavours, and 2 particle-antiparticle):

$$\epsilon = (A_\gamma + A_l + A_g + A_q) \times T^4 [\text{MeV}^4] \quad (12)$$

with  $A_\gamma=0.65$ ,  $A_l = 2.30$ ,  $A_g=5.26$  and  $A_q=10.36$ .

For a small size plasma (radius below  $10^{-10}$  m) or short lifetime, electromagnetic particles like photons and leptons could not reach thermalisation. They will be radiated by the thermalised medium but they will not be in equilibrium with the medium. Ignoring them, one gets  $\epsilon = 15.62 \times T^4 [\text{MeV}^4]$  for 3 flavors of massless quarks and 8 gluons (see the value of  $\epsilon_{SB}/T^4$  in Fig. 5).

## F. Probes of the QGP

### 1. Thermal radiation

Thermal radiation from a QGP will allow to study several properties of the QGP like its temperature  $T$ . On the surface of the QGP volume, photons<sup>9</sup> will escape. This is the thermal radiation.

As we have estimated for an ideal QGP, the partial pressure of these photons on the QGP surface, will be given by the expression  $p = \epsilon/3 = 0.22T^4$  and their energy distribution by the Planck law. In consequence the differential partial pressure  $dp/dE_\gamma$  in natural units will be :

$$\frac{dp(E_\gamma, T)}{dE_\gamma} = 0.034 \frac{E_\gamma^3}{\exp(E_\gamma/T) - 1} [\text{MeV}^3] \quad (13)$$

where  $E_\gamma$  is the photon energy in MeV. Considering massless particle and a QGP of a radius 7 fm and 10 fm/c lifetime, the thermal radiation spectrum is presented in Fig. 9

---

<sup>9</sup> but also the other fundamental particles.

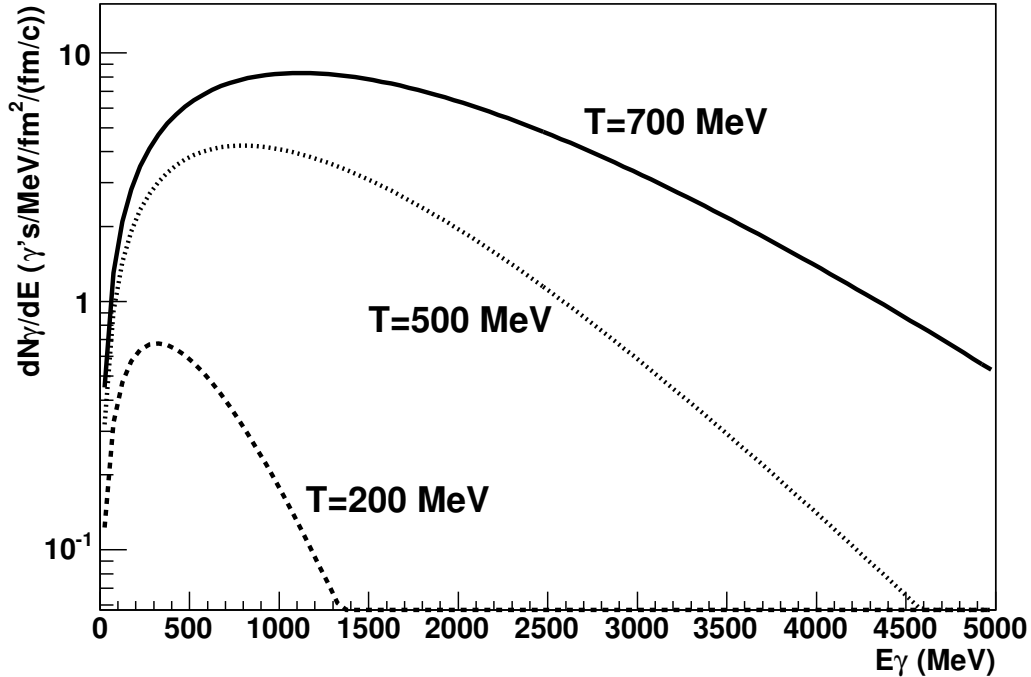


FIG. 9. Thermal photon production in a QGP of 7 fm radius and during 10 fm/c, as expected from a black-body radiation.

for temperatures of 200 MeV, 500 MeV and 700 MeV. The corresponding photon yields for energies above 1 GeV are 52, 4600 and 16000, respectively.

Obviously, the numerical example presented here is unrealistic since a 7 fm radius QGP will be transparent to photons. Under these conditions, the electromagnetic radiation of a thermalised QGP is not in thermal equilibrium with the medium which is producing it. Once a photon is produced, it will escape from the QGP, therefore the emission is from the volume and not from the surface as in the black-body radiation. The calculation of the thermal photon radiation from a QGP is complicated [Gelis 03, Arleo 03]. At first order, one could expect a reduction of the total number of photons emitted following the ratio of the strength of the strong and the electromagnetic forces  $\alpha_{QED}/\alpha_{QCD}$ . Only for large size QGP, with a radius above  $\sim 0.1$  Å, the black-body radiation model would become valid.

## 2. Screening of the colour potential between heavy quarks in the QGP

As we have already mentioned, the transition to the QGP only concerns the light quarks  $u$ ,  $d$  and  $s$ , for which the chiral symmetry is a good approximation. Since heavy quarks explicitly break the chiral symmetry, they are not directly concerned by the transition to QGP. In other words, the bound states of heavy quarks (quarkonia) are not necessarily melt in a QGP and they could exist as bound states. For this reason, these bound states become very interesting probes for measuring the temperature of the QGP [Matsui 86].

Let us see qualitatively which are the properties of a quarkonium embedded in a QGP.

Quarkonia are bound states between two heavy quarks  $Q\bar{Q}$ :  $c\bar{c}$  for the family  $\eta_c$ ,  $J/\psi$ ,  $\psi(2S)$ ,  $\chi_c$  ... and the states  $b\bar{b}$  for the family  $\Upsilon$ 's and  $\chi_b$ . The bound state  $t\bar{t}$  has not been experimentally observed and it will surely not exist due to the short lifetime of the top

quark. Finally, one should note that the hadronic states  $c\bar{b}$  ( $\bar{c}b$ ) will have similar properties as quarkonium, although their decay should be similar to that of a  $B$  hadron. In vacuum, the quarkonium spectrum can be described via non relativistic models based on a potential interaction like:

$$V(r) = \sigma r - \frac{\alpha}{r} \quad (14)$$

where  $\sigma$  represents the string tension  $Q\bar{Q}$  and  $\alpha$  is a Coulombian-like constant [Matsui 86]. For simplicity, let us assume that the potential is only Coulombian, so  $\sigma = 0$ .

If the  $Q\bar{Q}$  state is embedded in a QGP at a temperature  $T$ , the interaction potential between the heavy quarks will be affected by the presence of the free colour charges in the QGP. This is the screening of the potential. This phenomenon is well known in electromagnetic plasma. In the plasma, the Coulombian potential has to be replaced by a potential with a screening constant:

$$V(r) = -\frac{\alpha}{r} \times e^{(-r/\lambda_D)} \quad (15)$$

where  $\lambda_D$  is the Debye length. Let us assume that the average distance between the heavy quarks in a 1S quarkonium state ( $J/\psi$  or  $\Upsilon(1S)$ ) can be estimated by the Bohr radius expression:

$$r_B = \frac{1}{\alpha m_Q}. \quad (16)$$

As a numerical example, one can consider for the  $J/\psi$   $m_c=1250$  GeV and  $\alpha(m_c) = 0.36$  [Beringer 12], so  $r_B = 0.44$  fm. For the  $\Upsilon(1S)$ ,  $m_c=4200$  GeV and  $\alpha(m_b) = 0.22$  [Beringer 12], so  $r_B = 0.22$  fm.

If  $r_B \ll \lambda_D$ , the potential between the heavy quarks can be considered as a Coulombian potential and the bound state exhibits the same properties in the QGP as in the vacuum. However, if  $r_B \geq \lambda_D$ , the quarkonium properties will be modified by the medium, and it could happen that the quarkonium becomes an unstable state and therefore would melt. For electromagnetic plasmas, the Debye length depend on the temperature of the plasma and the charge density  $\rho$  [Stocker 99]:

$$\lambda_D = \sqrt{\frac{T}{8\pi\alpha\rho}} \quad (17)$$

Assuming that the previous expression is also valid for the QGP<sup>10</sup> and an ideal ultra-relativistic gas  $\rho \propto T^3$ , one obtains :

$$\lambda_D \sim \frac{1}{\sqrt{8\pi\alpha}T}. \quad (18)$$

And therefore, the quarkonium could be melt for temperature above  $T_d$ :

$$T_d \sim \frac{1}{\sqrt{8\pi\alpha(T)}r_B}. \quad (19)$$

For  $\alpha(T) \sim 0.2$ , one obtains that  $T_d \sim 200$  MeV ( $1.3T_c$ ) for the  $J/\psi$  and  $T_d \sim 400$  MeV ( $2.6T_c$ ) for the  $\Upsilon(1S)$ . Assuming that for 2S states the  $r_B$  would be twice larger, one would conclude that the dissociation temperature for  $\Psi'$  is  $\lesssim T_c$  and for  $\Upsilon(2S)$  similar to that of  $J/\psi$ .

Of course, these calculations are qualitative and obtained without much detail, but they allow to show what is the role of parameters like the mass of the quarkonium and the

---

<sup>10</sup> This assumption is not justified, but the conclusions that will be obtained are still valid.



Bound state	$\chi_c$	$\psi'$	$J/\psi$	$\Upsilon(2S)$	$\chi_b$	$\Upsilon(1S)$
$T_d$	$\lesssim T_c$	$\lesssim T_c$	$\sim 1.2T_c$	$\sim 1.2T_c$	$\sim 1.3T_c$	$\sim 2.0T_c$

TABLE II. Upper bound of dissociation temperatures  $T_d$  of quarkonium states in units of the QGP transition temperature  $T_c$  obtained by A. Mocsy and P. Petreczky in [Abreu 08].

strength of the interaction. This explains why  $\psi(2S)$  resonance is easily melt with respect to  $J/\psi$  and why  $\Upsilon(1S)$  would melt at higher temperatures than that of  $J/\psi$ . You will find a rigorous calculation of an upper bound of the dissociation temperature of quarkonium in the contribution of A. Mocsy and P. Petreczky in the reference [Abreu 08]. Their dissociation temperatures are quoted in table II.

### 3. Parton - QGP interaction

The QGP could also be studied via its tomography using high energy partons. QCD predicts that high energy partons will lose energy via gluon radiation when crossing the QGP. The order of magnitude of the parton energy-loss in QGP would be about  $\Delta E \sim 1$  GeV/fm and it is expected to be proportional to the gluon density. In addition QCD also predicts that the formation length of the radiated gluon will be larger than the average distance between the gluons in the QGP (interaction centres of the incident high energy parton). As a consequence several interaction centres will participate in the gluon emission from the parton, and the amplitude from the interaction centres will interfere (this phenomenon is called Landau-Migdal-Pomeranchuk effect) since the radiated gluon will be coherently emitted along all its formation length. For this reason for QGP thicknesses about 1-3 fm, the  $\Delta E$  should be proportional to the square of the transversed path length in the QGP [Baier 97, Zakharov 97]:

$$\Delta E \sim \alpha_s \times C_R \times \hat{q}(\rho_g) \times L^2 \quad (20)$$

where  $\alpha_s$  is the strength of the strong interaction,  $C_R$  is the colour charge factor  $\hat{q}$  is the transport coefficient which depends on the gluon density ( $\rho_g$ ) of the QGP and  $L$  is the thickness of the QGP.

The energy lost will depend on the nature of the parton:

- Gluons will exhibit larger energy-loss per unit of length than that of quarks. A relative factor 9/4 due to the colour charge, is associated to the gluonsstrahlung mechanism from a gluon with respect to that from a quark [Peigné 06].
- Heavy quarks are expected to lose less energy than light quarks, due to the absence of gluon radiation at forward angles, below  $\theta < M/E$ , where  $M$  is the quark mass and  $E$  its energy [Dokshitzer 01]. This phenomenon, predicted by the QCD, is called dead-cone effect. The dead-cone effect should become measurable for beauty quarks, whereas this effect should remain relatively small for charm quarks. Moreover, elastic collisions with partons in the QGP could also contribute to the energy-loss of heavy quarks in the QGP. Finally the hadronization time scale for heavy quark hadronization increases due to its larger mass and it could occur, namely for the beauty, that hadronization takes place when the heavy quark is still traversing the QGP.

One can wonder if other high-energy elementary particles like photons, electrons, electroweak bosons etc... could also be used to study the QGP. Photons and electrons will only interact electromagnetically and they should lose energy like in ordinary matter via bremsstrahlung emission and the production of electrons and positron pairs. However, the expected energy-loss is relatively small for QGP of a radius of tens of femtometers, about

$\sim 1\%$  of the energy of the particle [Peigné 06]. In the case of electroweak bosons, they will decay quickly due to their short lifetime and only their daughter particles will interact with the QGP.

### III. HEAVY ION COLLISIONS AND HEAVY ION ACCELERATORS

The study of hadronic matter in the laboratory is one of the challenges of experimental nuclear physics since the eighties. Today, the unique experimental method consists in accelerating and colliding two heavy nuclei. In laboratories like CERN (Geneva, Switzerland), BNL (New York, USA), GSI (Darmstadt, Germany), and GANIL (Caen, France), nuclei are accelerated at energies that range from MeV to TeV beam energies. Depending on the center-of-mass energy of the collision, different domains of the phase diagram of hadronic matter can be studied. Before the collision, the nucleus-nucleus system is out of equilibrium. During the collision, the strong interaction between the constituents may dissipate a fraction of the available center of mass energy into the internal degrees of freedom of the system, and hopefully, a microscopic drop of hot hadronic matter could be created in the laboratory. The pressure gradient between the drop and the surrounding vacuum would be incredibly high and the drop will suffer a dramatic expansion against the vacuum. The temperature of the system will change during the expansion and a series of ephemeral thermodynamical states will be created. The complexity of this dynamical evolution of the system makes much more difficult the study of the intrinsic properties of the hadronic matter and a rigorous methodological approach has to be undertaken:

- **Collision dynamics.** The systematic study of the different colliding systems, center of mass energies and impact parameter will be of vital importance;
- **Experimental probes.** This implies that one can detect, identify and measure the kinematic properties of all the particles produced in the nucleus-nucleus collisions. This has not been always possible, and only large scale experiments in colliders like STAR, PHENIX, ATLAS, ALICE or CMS are able to perform such a complete measurement. This is the only way to measure all the experimental probes, like particle multiplicity, light and strange hadron yields, transverse momentum and rapidity distributions, hadron correlations, azimuthal asymmetries, heavy quarks, quarkonia, direct photons, jets, dijets, electroweak bosons, photo-jet and electroweak bosons-jet correlations, etc ...
- **Experimental probes in cold nuclear matter.** In addition, one has to study the experimental probes when the microscopic drop of hot hadronic matter is not created, namely, in peripheral collisions and/or induced-proton collisions;
- **Global interpretation.** The results obtained have to be interpreted in one single scenario that explains coherently the whole phenomenology of experimental results.

In order to create a drop of QGP in the laboratory, energy densities of about  $1.0 \text{ GeV/fm}^3$  have to be reached. Nucleus-nucleus collisions at relativistic energies have become a unique experimental method. Naively, one could assume that all the available energy in the center-of-mass is dissipated, during the collision, into the internal degrees of freedom of the nucleus-nucleus system. The latter statement is certainly a bad hypothesis since anyone will expect that a non negligible fraction of the available energy in the center-of-mass will not be dissipated to create hot matter. But this hypothesis allows to estimate the beam energy below which, the QGP cannot be formed. Under this hypothesis, the energy density of the drop will approximately be given by

$$\epsilon \approx \frac{\sqrt{2E_b \times m \times A}}{V} \quad (21)$$

where  $m$  is the mass of the nucleon,  $E_b$  is the beam energy in the reference system where one of the nucleus is at rest,  $A$  the atomic number and  $V$  the initial volume of the system. Assuming:

$$V \approx 4/3\pi \times (1.124)^3 \times A \text{ [fm}^3\text{]}, \quad (22)$$

we conclude that for beam energies  $E_b$  below  $\sim 20$  GeV per nucleon (that is, a center-of-mass energy below  $\sqrt{s_{NN}}=6$  GeV per nucleon pair) the energy available in the center of mass is insufficient to heat a nucleus to energy densities above  $1 \text{ GeV/fm}^3$ . It seems hardly possible that a drop of QGP could be then formed. Even at  $E_b \sim 20$  GeV per nucleon, the stopping power of nuclear matter would not be strong enough to stop both nuclei, and in consequence only a fraction of the initial beam energy could be dissipated into the internal degrees of freedom of the system. Therefore  $E_b$  noticeably larger than 20 GeV per nucleon would be needed to reach the critical density of the QGP phase transition.

At the beginning of the 80's, the American physicist J.D Bjorken imagined a scenario where the QGP would be efficiently formed. He described what would be the initial energy density and its evolution with time [Bjorken 83]. As we will see later, one of the hypothesis of this scenario is only corroborated for  $E_b$  larger than  $\sim 250$  GeV, that is an available energy in the center of mass larger than 25 GeV per nucleon pair. In addition, the QGP would be formed at baryonic potentials close to zero under this scenario.

Therefore, it remains an open question whether the critical energy density could be reached or not, in the intermediate domain between  $E_b=20\text{-}250$  GeV ( $\sqrt{s_{NN}}=6\text{-}25$  GeV). As I will mention later, the results from the SPS experimental heavy ion program (1986-2000) at  $\sqrt{s_{NN}}=17\text{-}19$  GeV, hinted at the existence of a new state of matter in which quarks, instead of being bound up into more complex particles such as protons and neutrons, are liberated to roam freely.

### A. The Bjorken scenario of heavy ion collisions at ultra-relativistic energies

At ultra-relativistic energies, nuclei are seen as pancakes in the center-of-mass system, due to the Lorentz contraction. The crossing time of the nuclei can be estimated as

$$\tau_{cross} = 2R/\gamma, \quad (23)$$

where  $\gamma$  is the Lorentz factor and  $R$  the radius of the nuclei.

Bjorken assumed the following hypothesis:

- The crossing time  $\tau_{cross}$  is smaller than the time scale of the strong interaction. The latter can be estimated as  $\tau_{strong} \sim 1/\Lambda_{QCD} \sim 1 \text{ fm}/c$ . For a nucleus-nucleus collision,  $\tau_{cross}$  is larger than  $\tau_{strong}$  only if  $\gamma < 12$ . That is an energy in the center of mass above  $\sqrt{s_{NN}} > 25$  GeV (so  $E_f > 250$  GeV for a fixed-target experiment)<sup>11</sup>. Under this hypothesis, the particles generated by the strong interaction between the nucleon partons, are created once the nuclei have already crossed each other.
- The distribution of the particle multiplicity as a function of the rapidity is assumed to be uniform. This is partially verified experimentally in Au-Au collisions at RHIC [PHOBOS 06], in proton-antiproton collisions at Tevatron [CDF 90], and at SPS energies [Bjorken 83]. This condition ensures a rapidity symmetry of the system, allowing to create a uniform energy density in different rapidity slices, which simplifies considerably the description of the hydrodynamical evolution of the system.

<sup>11</sup> To be noted that only RHIC and LHC colliders validate this hypothesis with  $\gamma$  values of 100 and 1376 (and 2750 after year 2015) respectively.

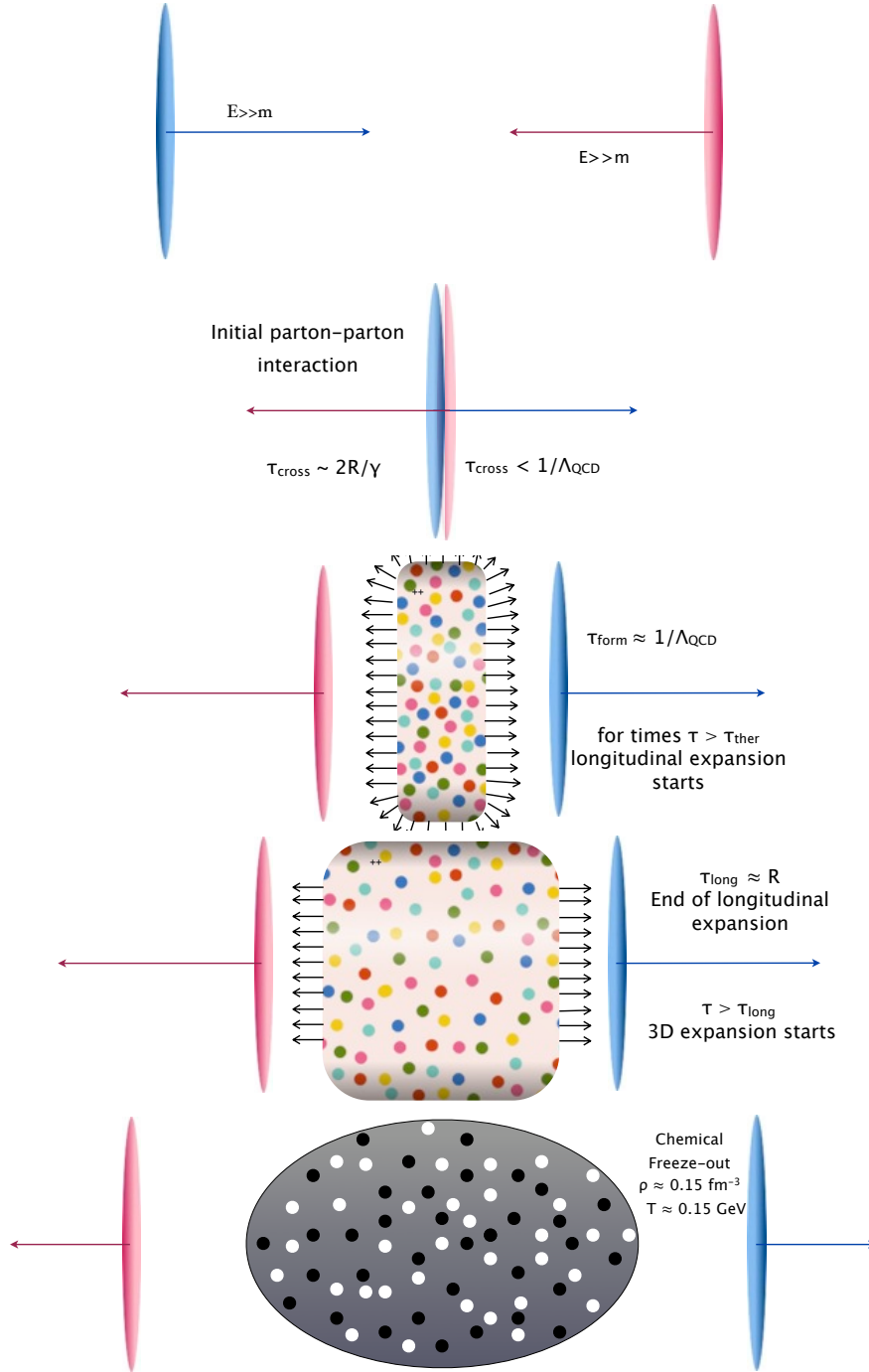


FIG. 10. Bjorken scenario [Bjorken 83] for the formation of hot QCD matter. After a formation time  $\tau_{\text{form}}$  a volume with a high energy density is created. After equilibration at  $\tau_{\text{ther}}$ , the evolution of the hot QCD matter follows the laws of the relativistic hydrodynamics. First, there is a longitudinal expansion until the system reaches a longitudinal size close to its transverse size, then a tridimensional expansion starts until the density is so low that no more inelastic (elastic) collision takes place. The system reaches then the so called chemical (kinetically) freeze-out. Finally all the particles will fly decaying to their daughter particles or reaching the detector. Typically only charged pions, charged kaons, protons, neutrons, photons, electrons and muons will reach the detectors.

Let's consider the volume centred in the nucleus crossing plane, at a time  $\tau$  after the nucleus crossing. This volume has a cylindrical shape with a thickness  $2\Delta d$  along the beam axis direction and a radius  $R \sim 1.124A^{1/3}$  in the transverse plane. This volume will contain all the particles produced with a speed along the beam axis (z axis) below  $\beta_z \leq \Delta d/\tau$ . Since  $\beta_z = \tanh(y) \sim y$  for  $y \rightarrow 0$ , the rapidity range  $\Delta y$  around  $y = 0$  of particles with a  $\beta_z \leq \Delta d/\tau$  will be

$$\Delta y = \frac{2\Delta d}{\tau}. \quad (24)$$

and the total energy in the volume considered will be :

$$E = \left. \frac{dE}{dy} \right|_{y=0} \times \frac{2\Delta d}{\tau}, \quad (25)$$

where  $dE/dy$  is the total energy created by the strong interaction between the nuclei at  $y=0$ . For other rapidity domains, the previous expression can be easily generalised replacing the total energy by the transverse energy  $E_T$ . Finally, we can calculate the energy density in the volume<sup>12</sup>:

$$\epsilon(y) = \left. \frac{dE_T}{dy} \right| \times \frac{1}{\pi R^2 \tau}, \quad (26)$$

which links the energy density with the transverse energy produced per unit of rapidity.

### 1. Formation.

The initial energy density can then be estimated assuming the time scale needed for the production of particles, as  $\tau_{\text{form}} \sim \tau_{\text{strong}} \sim 1 \text{ fm}/c$ <sup>13</sup>.

Bjorken estimated the energy density for heavy ion collisions at beam energies of the Sp $\bar{p}$ S collider at CERN, that were  $\sqrt{s_{\text{NN}}} \sim 500 \text{ GeV}$  per nucleon pair<sup>14</sup>, and he obtained that the initial energy density were about 2-20 GeV/fm<sup>3</sup>, largely above the critical energy density to form the QGP. One can redo the exercise for heavy ion collisions at Tevatron energies ( $\sqrt{s_{\text{NN}}} \sim 1.8 \text{ TeV}$  [CDF 88, CDF 90]), and then the initial energy density would be 4-30 GeV/fm<sup>3</sup>.

Note that in Fig. 10 only hot matter created around mid-rapidity and its evolution is presented. Indeed one should keep in mind that the hot hadronic matter is created in the full rapidity range where the particle density is high enough to reach equilibrium. At RHIC energies, this is about 5 units of rapidity and at LHC energies about 8 units of rapidity. In the laboratory system, the hot matter slices at larger rapidities are indeed narrower due to the Lorentz contraction.

### 2. Thermalisation.

The particles produced inside the volume considered will interact. At these energy densities, and assuming a mean energy  $\langle E \rangle = 500 \text{ MeV}$ ,  $\epsilon/\langle E \rangle \sim 8 - 60$  particles per fm<sup>3</sup> will be reached. The average path length of particles inside the volume can be estimated as  $\lambda \sim 0.02 - 0.12 \text{ fm}$ , if one assumes an interaction cross-section of 10 mb. One could hope

<sup>12</sup> There is a factor 2 difference with respect to equation (3) in the original publication of Bjorken [Bjorken 83]. It is a known typo error in the original publication.

<sup>13</sup> Other estimates that provide smaller  $\tau_{\text{strong}}$  in the range 0.2-0.5 fm/c can be foreseen [PHENIX 05a].

<sup>14</sup> The energy of the collider Sp $\bar{p}$ S is close to the available energies at RHIC: 200 GeV per nucleon pair

that the system will thermalise at a time  $\tau = \tau_{ther}$ . Note that this is a strong assumption that must be i) validated by the experimental results and ii) supported by theoretical calculations. Experimental results seem to agree with the assumption of a fast thermalization of the system, but the theory has not been able to explain how thermal equilibrium could be reached in such a short time scale. This reminds a fundamental question to be answered and it is still a challenge for QCD theory to describe the first instants of the nucleus-nucleus collision at ultra-relativistic energies. In principle, the initial state of the nucleus-nucleus collision is characterised by the interaction of two high-density gluon clouds. In this respect, classical limits of the QCD theory (like the Colour Glass Condensate [Gelis 11]) seem to be the best theoretical tool to study this problem. The typical Bjorken  $x$  of the two gluon clouds is  $\langle x \rangle \sim 10^{-2}$  at RHIC and  $\langle x \rangle \sim 10^{-3}$  at the LHC

### 3. Longitudinal expansion.

At stages  $\tau \geq \tau_{ther}$  the system should evolve like a fluid, following the laws of the relativistic hydrodynamics. First a longitudinal expansion will take place since the pressure gradient in the beam direction will be larger than that in the transverse plane. It is expected that the energy density will evolve as  $\epsilon \sim 1/\tau^n$  with  $1 \leq n \leq 4/3$ , which is obtained from the hydrodynamic law [Bjorken 83]

$$\frac{d\epsilon}{d\tau} = -\frac{\epsilon + p}{\tau}. \quad (27)$$

and for an ideal ultra-relativistic gas, this becomes  $\epsilon = 3p$  and thus  $n=4/3$ . The longitudinal expansion stays as a good approximation for stages  $\tau \leq \tau_{long} \sim R$ .

### 4. 3D expansion and freeze-out phase.

For stages  $\tau \geq \tau_{long}$  the system will evolve via a 3 dimensional expansion until the freeze-out stage is reached. At freeze-out, particle density is low enough to assume that particles do not interact, travel in the vacuum, can decay and finally reach the detector. Naively, the freeze-out will take place when the average path length of particles is similar to the size of the system  $\lambda \sim R$ . For a cross-section of 10 mb, this corresponds to 0.15 particles per fm<sup>3</sup> and therefore an energy density of

$$\epsilon_{gel} \sim 0.15 \text{ fm}^{-3} \times 0.5 \text{ GeV} \sim 0.075 \text{ GeV/fm}^3. \quad (28)$$

It is then expected that the freeze-out takes place as a hadron gas phase. Note that for a freeze-out temperature of  $T_{gel} = 150 \text{ MeV}$ , one gets  $\epsilon/T^4 \sim 1.2$ , which fits pretty well with the prediction of lattice QCD calculations of Fig. 5. Finally it is worth mentioning that elastic cross-section is larger than inelastic one and one expects to observe two different freeze-out stages: chemical and kinetic freeze-out ones.

## B. Heavy ion accelerators and colliders

Developments in heavy ions beams at ultra-relativistic energies have been performed in parallel as that at intermediate energies, since the main technical limitation was the ion source and the heavy-ion injection at low energies. The first heavy ion beams at relativistic energies were produced at AGS (BNL, USA) and at SPS (CERN, Switzerland) in the 80's. The energy in the centre of mass was 5 and 18 GeV per nucleon pair, respectively. The first

heavy ion collider was RHIC, built at BNL, which provided the first Au-Au collisions at  $\sqrt{s_{NN}}=130$  GeV in June 2000 and reached in 2001 its nominal energy of  $\sqrt{s_{NN}}=200$  GeV. Finally, LHC provided its first heavy ion collisions of Pb beam at  $\sqrt{s_{NN}}=2760$  GeV, a 14-fold increasing step with respect to RHIC, in November 2010 and hopefully this will turn into a 28-fold factor (5500 GeV) from 2015 onwards. Today, RHIC and LHC are developing their heavy ion programs which are foreseen until 2025.

### 1. The Alternating Gradient Synchrotron at BNL

The AGS synchrotron was built in 1957 and allows the acceleration of high intensity proton beams at 33 GeV. Several Nobel prizes were obtained (1976, 1980 and 1989) linked to discoveries at AGS:  $J/\psi$  discovery in 1974, observation of the CP violation of the weak interaction in 1963 and the discovery of the muonic neutrino (1962). Since 1986, the AGS synchrotron has been used to accelerate Si ions at energies of 14 GeV per nucleon, after the construction of the beam line to inject heavy ions in AGS from the Tandem Van de Graaf (built in 1970). The Si beam from the tandem has an energy of 6.6 MeV per nucleon. The construction of the AGS booster in 1991 allowed to increase the AGS beam intensity and to accelerate heavier ions like Au up to 11 GeV per nucleon. Negative  $Au^-$  ions are extracted from the source and accelerated by the tandem to 1.17 MeV per nucleon and stripped to a beam of  $Au^{+32}$ . This beam is then injected in the AGS booster where the Au ions are accelerated to 90 MeV/nucleon. Finally the Au beam is stripped and injected into AGS where it is accelerated to the nominal energy of 11 GeV per nucleon. For 14 years, several fixed target heavy-ion experiments took place, like E866, E877, E891, E895, E896, E910, E917 to study the hadronic matter at high temperature<sup>15</sup>.

### 2. The Super Proton Synchrotron at CERN

The SPS was built in 1976, allowing for proton acceleration until 500 GeV. First, protons are accelerated by a linear accelerator called LINAC2, and then injected into the booster of the PS (Proton Synchrotron) and finally they are injected into the SPS to reach their nominal energy of 500 GeV<sup>16</sup>. From 1986, the new electron-cyclotron resonance (ECR) ion source allowed the injection of multi charged heavy ions in the CERN accelerator system (LINAC3, PS booster, PS and SPS). The beam leaving from an ECR ion source containing a Pb plasma, has an energy of 2.5 KeV per nucleon with an ion charge  $Q = +27$ , and they are injected in the LINAC3 linear accelerator reaching a beam energy of 4.2 MeV per nucleon. Then the beam is stripped via a thin C layer 1  $\mu m$  thick, and becomes a  $^{+53}Pb$  beam, which is injected in the PS booster and PS accelerator, reaching an energy of 4.25 GeV per nucleon. The Pb ions are then fully stripped in an aluminium layer of 1 mm thick, and they are injected in SPS to reach an energy of 158 GeV per nucleon. This beam is finally directed to the experimental fixed-target halls in SPS north area (NA) in France or SPS west area (WA) in Switzerland, where heavy ion collisions at  $\sqrt{s_{NN}}$  take place. In addition to Pb, other ions have been also accelerated at SPS. At the beginning of the SPS heavy ion program, beams of O and S were accelerated at energies about 60 and 200 GeV per nucleon, and in the last days In ions were used for the NA60 experiment. During 20

<sup>15</sup> Note that it is not clear the AGS could form deconfined matter since the initial energy density could be below 1 GeV/fm<sup>3</sup>.

<sup>16</sup> Initially the SPS was a proton accelerator. But SPS became a proton-antiproton collider with to the additional injection of antiproton beam. The latter was attainable thanks to the stochastic-cooling technique in the SPS ring. The first collisions  $p\bar{p}$  in SPS took place in 1981 at a center of mass energy of 520 GeV. Two years later, the electroweak bosons were discovered by the UA1 and UA2 experiments. The stochastic-cooling and the discovery of the W, and Z bosons was awarded with the Nobel prize of physics in 1984.

years, many heavy ion experiments were built, installed and contributed to the SPS heavy-ion physics programme: WA80, WA93, WA98, WA85, WA94, WA97, NA57, Helios-2, NA44, CERES, Helios-3, NA35, NA49, NA36, NA52, NA38, NA50 et NA60. In 2000, the analysis and interpretation of the obtained experimental results was almost finished and a CERN press released was organised<sup>17</sup>. They announced that the physical results of the heavy ion fixed-target SPS experiment NA44, NA45, NA49, NA50, NA52, WA97 / NA57 and WA98 hinted at the existence of a new state of matter in which quarks, instead of being bound up into more complex particles such as protons and neutrons, were liberated to roam freely.

### 3. *The Relativistic Heavy Ion Collider at BNL*

The first Au-Au collisions at 130 GeV per nucleon pair took place in June 2000 in RHIC at BNL (USA). It was the first collider ever built for heavy ions. AGS is the injector of RHIC, via a two Au beams at 9 GeV per nucleon which circulate in two different rings in opposite directions. In RHIC collider, 60 beam bunches in each ring are accelerated to the nominal energy of 100 GeV per nucleon and stored in two rings of 3.85 km perimeter length. The bunches of the two beams can collide in 4 interaction points along the RHIC ring, reaching nominal luminosities about  $2 \cdot 10^{26} \text{ cm}^{-2} \text{ s}^{-1}$ , that is a Au-Au collisions rate of 800 Hz. Recently, RHIC has been upgraded and is able to provide 5-10 times more instantaneous luminosity. In addition, RHIC collider allows to study collisions of polarised protons at 500 GeV, and collisions of d-Au, Cu-Cu, Au-Au and U-U in the energy range 20-200 GeV per nucleon pair. Since 2000, the four experiments at RHIC: STAR, PHENIX, PHOBOS and BRAHMS have developed a high quality physics program, producing a huge amount of experimental results. Today only the two major experiments: PHENIX and STAR are still active and taking data.

### 4. *The Large Hadron Collider at CERN*

The LHC at CERN uses SPS as injector. SPS was upgraded to generate a Pb ions beam at 177 GeV per nucleon, that are accelerated to a beam energy of 1.38 TeV. LHC provided the first Pb-Pb collisions at 2.76 TeV in November 2010, increasing by a factor 14 the centre-of-mass energy at RHIC. In November 2011 a new heavy-ion run took place at the same energy and the nominal instantaneous luminosity was reached,  $\sim 5 \cdot 10^{26} \text{ cm}^{-2} \text{ s}^{-1}$ . It is expected that the nominal energy, 5.5 TeV per nucleon pair, will be reached after the long shutdown during 2013-2014. In principle the instantaneous luminosity at LHC and beam lifetime is limited by the huge cross-section of i) electromagnetic production of electron-positron pairs where the electron is captured by the Pb ions and ii) electromagnetic excitation of the Pb nucleus giant resonance, leading to neutron emission. Both processes are responsible for the Pb beam loss at LHC energy. LHC will be upgraded in 2018 to increase by a factor 10 the instantaneous luminosity of the Pb-Pb collisions. At LHC, three of the four LHC experiments participate in the heavy ion program: ALICE, ATLAS and CMS. ALICE is the only LHC experiment devoted to the study of QGP. LHC will provide the first proton-Pb collisions at the beginning of 2013.

---

<sup>17</sup> <http://press.web.cern.ch/press/PressReleases/Releases2000/PR01.00EQuarkGluonMatter.html>.



#### IV. SOME BASES ABOUT COLLISION CENTRALITY AND THE NUCLEAR MODIFICATION FACTOR

In Fig. 10, the Bjorken scenario is presented for a central (zero impact parameter,  $b$ ) collision is presented. Actually, collisions at any impact parameter between  $b = 0$  and  $b = R_1 + R_2$  (the sum of the nuclear radius) could occur in the laboratory. It turns out that most of the collisions are indeed peripheral collisions, since the probability density is proportional to  $b$ . In experiments, the centrality of the collision can be estimated on an event-by-event basis via any observable  $\mathcal{C}$  that monotonically varies with the impact parameter of the collision. The observable  $\mathcal{C}$  can be the charged particle multiplicity or transverse energy in a given pseudo-rapidity interval, or energy at zero degree (at rapidities close to the beam rapidity), etc... Let us assume that i)  $f(\mathcal{C})$  represents the distribution of the observable  $\mathcal{C}$  for a sample of non biased nucleus-nucleus collisions, that ii)  $\mathcal{C}(b) \geq 0$  and that iii)  $\mathcal{C}(b=0) = 0$ . The centrality class  $n\%$  of the most central collisions consists of nucleus-nucleus collisions where the observable  $\mathcal{C} \in (0, \mathcal{C}_n)$  and

$$n = 100 \times \frac{\int_0^{\mathcal{C}_n} f(\mathcal{C}) d\mathcal{C}}{\int_0^\infty f(\mathcal{C}) d\mathcal{C}} \quad (29)$$

The  $n\%$  most central collisions are usually referred to as the centrality class 0- $n\%$ . Therefore the reaction class  $m\%-n\%$  ( $m < n$ ) is defined by the collisions where the observable  $\mathcal{C} \in (\mathcal{C}_m, \mathcal{C}_n)$ .

One of the experimental methods to quantify the nuclear medium effects in the production of a given observable (Ob) is the measurement of the nuclear modification factor ( $R_{AA}^{\text{Ob}}$ ) in nucleus-nucleus (A-A) collisions, defined as:

$$R_{AA}^{\text{Ob}} = \frac{Y_{AA}^{\text{Ob}}}{\langle N_{coll} \rangle Y_{pp}^{\text{Ob}}} \quad (30)$$

where  $\langle N_{coll} \rangle$  is the average number of binary nucleon-nucleon collisions<sup>18</sup> and  $Y_{AA}^{\text{Ob}}$  ( $Y_{pp}^{\text{Ob}}$ ) is the invariant yield of the observable Ob in A-A (pp) collisions at a given (same) center-of-mass energy. In the absence of nuclear matter effects, the nuclear modification factor should be equal to unity for experimental observables commonly called *hard probes* (large  $p_T$  particles, jets, heavy-flavour, etc). A similar factor  $R_{pA}^{\text{Ob}}$ , measured in p-A collisions, is crucial in order to disentangle hot and cold nuclear matter effects in A-A collisions.

#### V. BRIEF SUMMARY OF THE EXPERIMENTAL RESULTS AT RHIC AND AT THE LHC

Due to a lack of time, I have not been able to complete satisfactorily these proceedings. For this reason, I am giving here a brief summary of the main results from RHIC (12 years of heavy ion programme) and from LHC (after the two first years of heavy ion programme).

##### A. Initial energy density

The multiplicity of charged particles  $dN_{ch}/d\eta$  was measured at RHIC [PHOBOS 00, PHOBOS 02, PHENIX 05a, PHENIX 05b] (as well as the transverse energy [PHENIX 01,

<sup>18</sup> The average number of binary nucleon-nucleon collisions can be estimated by the product of the average nuclear overlap function (of the nucleus-nucleus collision) and the inelastic proton-proton cross section [Miller 07, d'Enterria 03].

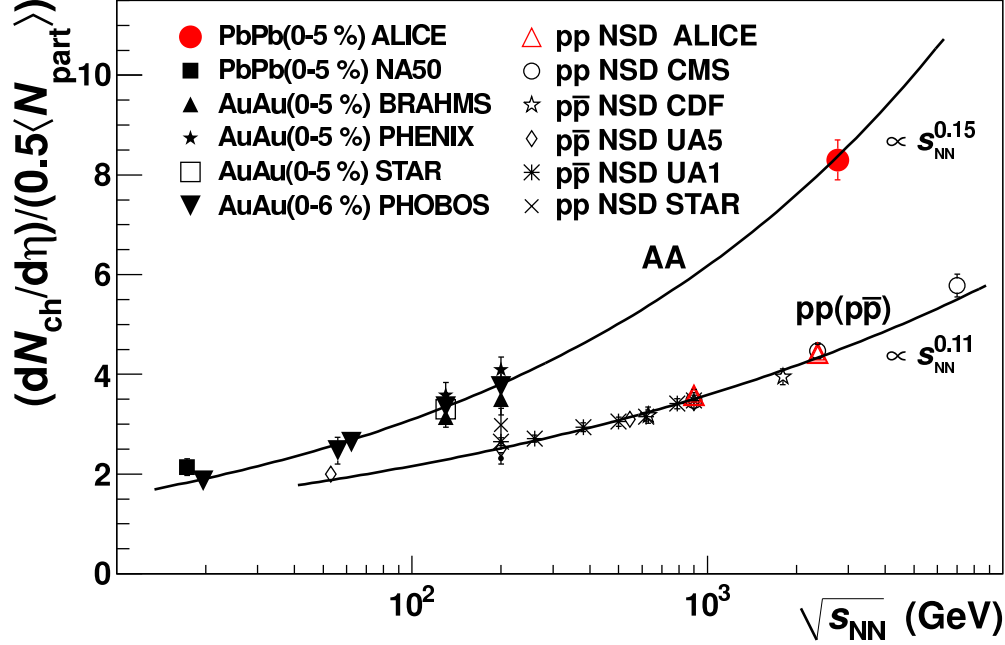


FIG. 11. Charged particle pseudo-rapidity density per participant pair for central nucleus-nucleus collisions. The solid lines  $\propto s_{\text{NN}}^{0.15}$  and  $\propto s_{\text{NN}}^{0.11}$  are superimposed on the diffractive pp collisions as a function of  $\sqrt{s_{\text{NN}}}$  heavy-ion and pp data, respectively. Figure 3 in reference [ALICE 10a].

STAR 04b]). The most central Au-Au collisions at 200 GeV generate more than 600 charged particles per unit of pseudo-rapidity at mid-rapidity, which should correspond to about 900 (charged and neutral) particles per unit of pseudo-rapidity<sup>19</sup>. Using the Bjorken model one can estimate that the initial energy density at mid-rapidity amounts to about 5-15 GeV/fm<sup>3</sup>. In addition the charged particle multiplicity remains constant within  $\sim 10\%$  for 5 units of pseudo-rapidity ( $|\eta| \lesssim 2.5$ ) [PHOBOS 11]. In the most central Pb-Pb collisions at 2.76 TeV, CMS has measured that transverse energy at mid-rapidity is about  $\sim 2$  TeV per unit of pseudo-rapidity [CMS 12b]. ALICE and ATLAS measured about  $\sim 1600$  charged particles per unit of pseudo-rapidity [ALICE 10a, ALICE 11a, ATLAS 12b] (see Fig. 11). Considering the increase of the mean hadron  $p_T$  at the LHC, the initial energy density at LHC is about three times larger than in Au-Au at RHIC top energy: 15-30 GeV/fm<sup>3</sup>. In both cases, the energy densities are several times larger than the critical energy density to form deconfined matter. Assuming that the system quickly equilibrates, the initial temperature could be estimated from the lattice QCD, assuming  $\mu_B \sim 0$ , (see Fig. 5) as

$$T^4[\text{MeV}^4] \approx \frac{200^3 \times 10^3}{12.5} \times \epsilon [\text{GeV}/\text{fm}^3] \quad (31)$$

which gives an estimate of the initial temperature of 240-320 MeV at RHIC top energy and 310-370 MeV at LHC 2.76 TeV energy.

## B. Equilibration

Integrated hadron yields at mid-rapidities were studied in both energy domains. It is observed that the hadron yield ratios can be successfully described by a statistical model

<sup>19</sup> Grosso-modo one assumes that the pions are the most abundant produced particles. Only the  $\pi^0$  is neutral, so the total number of particles per unit of rapidity can be estimated as  $600 \times 3/2$ .

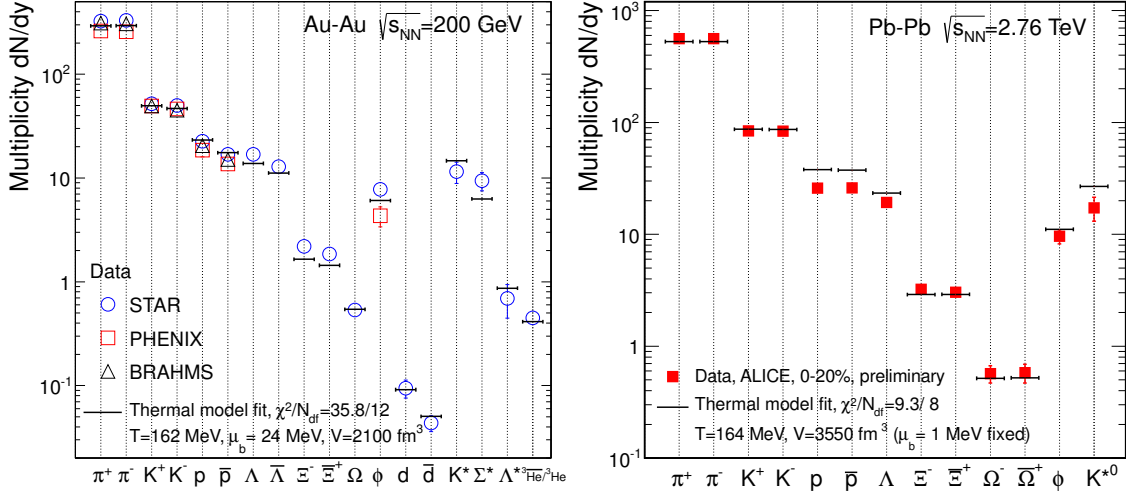


FIG. 12. *Left: Comparison of thermal model predictions with RHIC data. Right: Thermal model fits to ALICE data on hadron production in central Pb–Pb collisions. From reference [Andronic 12].*

[Andronic 04]. In this model, the expanding hot system hadronizes statistically at the freeze-out, and therefore the hadron yields are given by the following expression:

$$n_i = \frac{N_i}{V} = \frac{g_i}{2\pi^2} \int_0^\infty \frac{p^2 dp}{\exp[(E_i - \mu_i)/T] \pm 1} \quad (32)$$

with (+) for fermions and (−) for bosons,  $T$  is the temperature,  $N_i$  is the total number of hadrons of the species  $i$ ,  $V$  the total volume of the system,  $g_i$  is the isospin and spin degeneration factor,  $E_i$  the total hadron energy and  $\mu_i$  the chemical potential. Considering zero total strangeness and isospin of the system, one can consider  $\mu_i = \mu_b$  where  $\mu_b$  is the baryonic chemical potential. Therefore only two parameters are needed to predict the hadron yield ratios: the freeze-out temperature and the baryonic potential. The analysis of hadron yield ratios allows to extract a similar freeze-out temperature of  $\sim 160$  MeV at RHIC and at the LHC (see Fig. 12). The baryonic potential is  $\mu_b \sim 20$  MeV at RHIC and, as expected, a lower  $\mu_b$  at LHC, indeed close to zero [Andronic 09, Andronic 12]. The value of the temperature at chemical freeze-out is indeed very close to the phase transition temperature as predicted by lattice calculations presented in section II D. One should notice that, at LHC energies, proton and antiproton yields normalised to the pion yields exhibit an anomalous behaviour that has to be further investigated [Andronic 12].

The azimuthal distribution of particles in the plane perpendicular to the beam direction is an experimental observable which is also sensitive to the dynamics of the early stages of heavy-ion collisions. When nuclei collide at finite impact parameter (non-central collisions), the geometrical overlap region and therefore the initial matter distribution is anisotropic (almond shaped). If the matter is strongly interacting, this spatial asymmetry is converted via multiple collisions into an anisotropic momentum distribution [Ollitrault 93]. The second moment of the final state hadron azimuthal distribution with respect to the reaction plane is called the elliptic flow ( $v_2$ ):

$$E \frac{d^3 N}{d^3 \vec{p}} = \frac{1}{2\pi} \frac{d^2 N}{p_T dp_T dy} \left[ 1 + \sum_{n=1}^{\infty} \left\{ 2v_n \cos[n(\phi - \Psi_R)] \right\} \right] \quad (33)$$

where  $\Psi_R$  is the reaction plane, defined by the beam axis and the impact parameter.

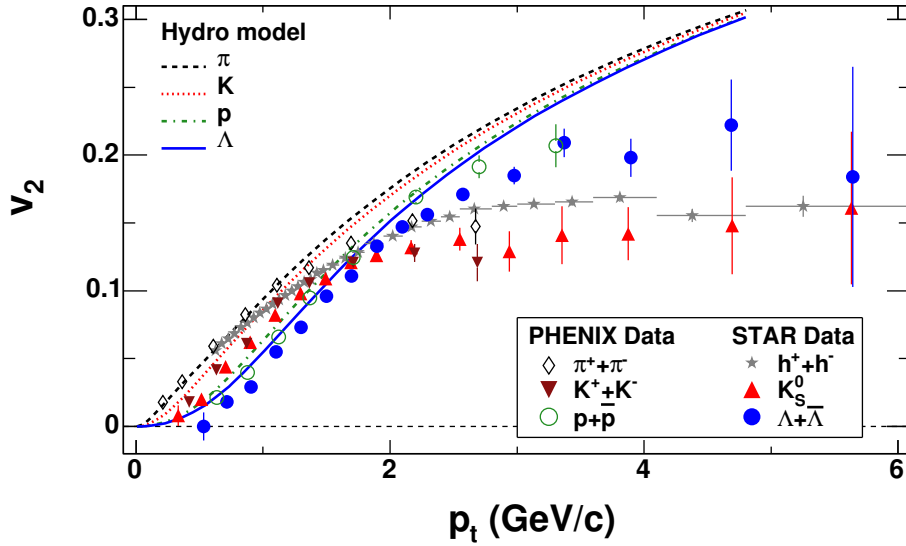


FIG. 13. The elliptic flow as a function of the transverse momentum measured by PHENIX and STAR collaborations for hadrons, pions, kaons, protons and Lambda baryons. Figure 10 in reference [STAR 05a].

The elliptic flow has extensively been studied at RHIC [STAR 01, STAR 05a, PHOBOS 07, PHENIX 09b, STAR 10a, STAR 12a] (see Fig. 13), and recently at LHC energies [ALICE 10b, ATLAS 12a, CMS 12a, ALICE 11b, ATLAS 12c]. Indeed the predictions from hydrodynamical models explain quite well most of the measurements of the elliptic flow of light hadrons at low  $p_T$  ( $p_T < 2 - 3$  GeV). The elliptic flow measurements have been one of the major observations at RHIC, evidencing that : i) the created matter equilibrates in an early stage of the collision, and then it evolves following the laws of the hydrodynamics; and ii) the formed matter behaves like a perfect fluid [PHENIX 05a, STAR 05b, PHOBOS 05, BRAHMS 05]. Furthermore, several works (see for instance reference [Nagle 10]) managed to extract values of transport properties, like the ratio of the shear viscosity over entropy from the experimental results. The conclusion was that the hot matter behaves as a perfect fluid and the mean free path of the constituents is close to the quantum limit. ALICE presented the first elliptic flow measurement at the LHC [ALICE 10b] in agreement with other LHC results [ATLAS 12a]. It was observed a similarity between RHIC and the LHC of  $p_T$ -differential elliptic flow at low  $p_T$ , which is consistent with predictions of hydrodynamic models ( $p_T \lesssim 2 - 3$  GeV/c). The elliptic flow is now being studied in much more details at LHC, for identified hadrons and as a function of the pseudo-rapidity (see for instance [ATLAS 12c]). Preliminary results on these topics are intriguing and it is certainly too early to conclude about their interpretation. In addition, the elliptic flow is being studied for the first time at very high  $p_T$ , (up to  $p_T \sim 40 - 60$  GeV/c) [CMS 12a]. Other moments of the hadron azimuthal distribution have been studied at RHIC and at the LHC [ALICE 11b, ATLAS 12a]. In particular non-zero  $v_3$ , was observed and it results from the fluctuations of the initial spatial distribution of the energy density. Complementarily to the  $v_2$ , the measurement of higher harmonics of the azimuthal distribution is also crucial to constrain the shear viscosity over entropy ratio in models.

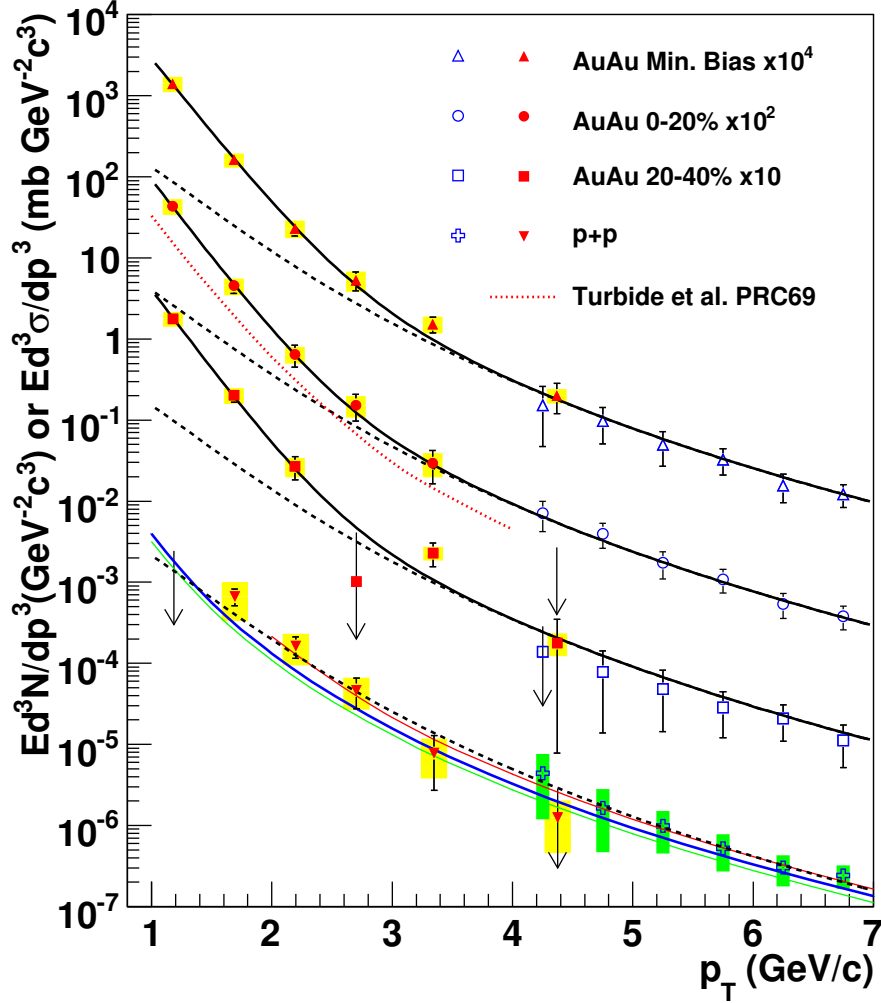


FIG. 14. Invariant cross section ( $pp$ ) and invariant yield ( $Au-Au$ ) of direct photons as a function of  $p_T$ . The three curves on the  $pp$  data represent NLO pQCD calculations, and the dashed curves show a modified power-law fit to the  $pp$  data, scaled by  $T_{AA}$ . The dashed (black) curves are exponential plus the  $T_{AA}$  scaled  $pp$  fit. The dotted (red) curve near the 0-20% centrality data is a theory calculation. Figure 3 in reference [PHENIX 10].

### C. Initial temperature

As we have seen in section II F 1, if QGP drop is formed, it should emit thermal radiation in the high energy  $\gamma$  domain. PHENIX collaboration have measured  $e^+e^-$  pairs with invariant masses below  $300 \text{ MeV}/c^2$  and  $1 \leq p_T \leq 5 \text{ GeV}/c$  in Au-Au collisions at 200 GeV [PHENIX 10]. The most central Au-Au collisions show a large excess of the dielectron yield (see Fig. 14). By treating the excess as internal conversion of direct photons, the direct photon yield is deduced. The yield cannot be explained by Glauber scaled NLO pQCD calculations. However, hydrodynamical models with an initial temperature of 300-600 MeV are in qualitative agreement with the data. The evidence for the production of *thermal* direct photons, with an initial temperature source above the QGP transition temperature

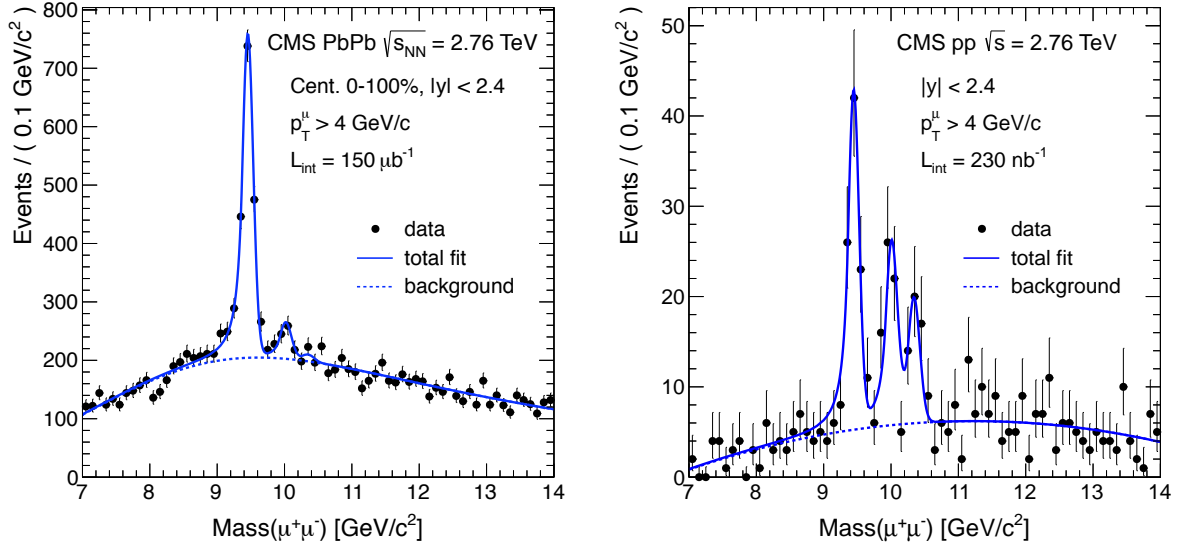


FIG. 15. Dimuon invariant-mass distributions in Pb-Pb (left) and pp (right) data at  $\sqrt{s_{NN}} = 2.76$  TeV. The solid (signal + background) and dashed (background-only) curves show the results of the simultaneous fit to the two datasets. Figure 1 in reference [CMS 12c].

represent an important experimental observation. Preliminary results from ALICE about thermal photon production in central Pb-Pb at 2.76 TeV are already available [Wilde 12]. The supposed thermal photon yield exhibits a 40% larger inverse slope at LHC than that at RHIC. The latter is in qualitatively good agreement with the expected relative increase of the initial temperature from RHIC to LHC energies.

Quarkonium was proposed as a probe of the QCD matter formed in relativistic heavy-ion collisions more than two decades ago. A familiar prediction, quarkonium suppression due to colour-screening of the heavy-quark potential in deconfined QCD matter [Matsui 86], has been experimentally searched for at the SPS and RHIC heavy-ion facilities.

CMS collaboration has performed the first measurement of the upsilon resonances ( $\Upsilon(1S)$ ,  $\Upsilon(2S)$  and  $\Upsilon(3S)$ ) at the LHC [CMS 11a, CMS 12g, CMS 12c]. The results indicate a significant decrease of the  $\Upsilon(2S)$  and  $\Upsilon(3S)$   $R_{AA}$  (see Fig. 15). The  $\Upsilon(1S)$   $R_{AA}$  is about 0.41 for the most central collisions. One should note that about 50% of the upsilon production in hadronic collisions is expected to result from the radiative decays of higher bottomonium resonances [Bedjidian 04]. If one assumes that high resonances are dissolved, one would expect to measure a nuclear modification factor for the  $\Upsilon(1S)$  about 0.5. The present measurement would be compatible with a formation of a QGP at the LHC at an initial temperature between 1.2-2.0 times the critical temperatures (see Tab. II), so absolute temperatures between 200-400 MeV. Since the melting temperatures of  $\Upsilon(2S)$  and  $J/\psi$  are expected to be similar (see Tab. II) one should expect a similar decrease of the  $J/\psi$   $R_{AA}$  at LHC energies.

The PHENIX experiment at RHIC reported the observation of  $J/\psi$  suppression in central Au-Au collisions at  $\sqrt{s_{NN}} = 200$  GeV (10 times higher than the maximum energy in the CM at SPS) [PHENIX 07, PHENIX 11b, PHENIX 12b]. Deuteron-gold collisions have been used to constrain cold nuclear matter (CNM) effects at RHIC energies [PHENIX 11a]. As a consequence,  $J/\psi$  suppression due to dissociation in QGP matter is roughly estimated to be 40-80% in central Au-Au collisions at RHIC energies. Since about 40% of the  $J/\psi$  yield results from the decays of higher resonances, it remains an open question whether the  $J/\psi$  is melt or not melt at RHIC energies. Finally, the STAR experiment has measured a smaller suppression at high transverse momentum ( $p_T \geq 5$  GeV/c) at mid-rapidity [STAR 09a,

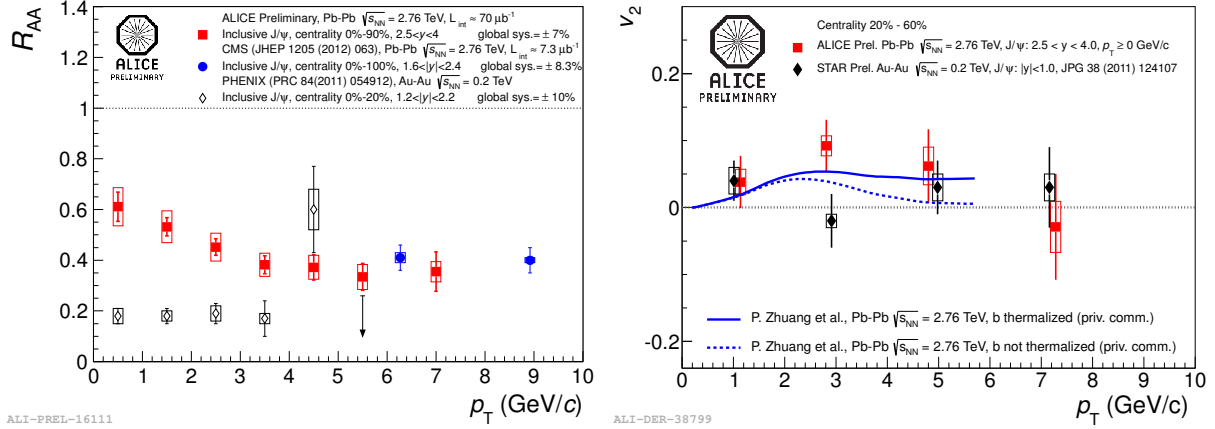


FIG. 16. *Left: ALICE  $p_T$  dependence of the inclusive  $J/\psi$   $R_{AA}$  measured in Pb-Pb collisions at  $\sqrt{s_{NN}} = 2.76$  TeV is compared to PHENIX and CMS measurements. Figure 2 in reference [Suire 12]. Right:  $J/\psi$  elliptic flow as a function of  $p_T$  in the centrality range 20-60% and in the rapidity range  $2.5 < y < 4$  (red squares). ALICE data are compared to STAR measurement performed in Au-Au collisions at  $\sqrt{s_{NN}} = 200$  GeV and in the rapidity range  $|y| < 1$  (black diamonds). ALICE data are compared with a transport model predictions. Figure 2 in [Massacrier 12].*

STAR 12c] although the experimental errors remain large.

#### D. The phase of deconfinement

At LHC energies, on average one  $J/\psi$  particle is expected to be produced in every central Pb-Pb collision, together with about 50-100  $c\bar{c}$  quark pairs. As suggested in 1988 [Svetitsky 88], under these conditions the charm quark yield per unit of rapidity could be large enough to enhance the charmonium production in later phases of the hot QCD-matter dynamical evolution, in particular when the energy density is low enough to enable the charmonium bound state to be formed [Braun-Munzinger 00, Grandchamp 04, Andronic 11]. The ALICE collaboration reported the first measurement of the  $J/\psi$  nuclear modification factor at LHC energies [ALICE 12d]. Contrary to the expectations from  $\Upsilon(2S)$  suppression,  $J/\psi$   $R_{AA}$  was found to be about 0.5 in the most central Pb-Pb collisions and does not exhibit a significant centrality dependence. In addition, the  $J/\psi$   $R_{AA}$  was found to be larger than that measured at RHIC. Contrary to RHIC observation, the  $J/\psi$   $R_{AA}$  is large at low  $p_T$  and then decreases with increasing  $p_T$  [Suire 12] (see Fig. 16 left). Finally, a hint of non-zero elliptic flow was also measured by the ALICE collaboration [Massacrier 12] (see Fig. 16 right). These experimental observations suggest that  $J/\psi$  production at LHC energies is governed, for an important part, by charm quark recombination processes. The production of charmonium in latter stages of the QGP evolution would certainly be a direct probe of the deconfinement phase.

Heavy-flavour hadrons, containing charm and beauty heavy quarks, are effective probes of the QGP. During the deconfined phase, low  $p_T$  heavy quarks will interact with the medium modifying its initial kinematical properties [van Hees 08, Gossiaux 09] and, in the extreme scenario, they could become fully thermalised. The first ALICE results on the nuclear modification factor  $R_{AA}$  for charm hadrons in Pb-Pb collisions indicate strong in-medium energy loss for charm quarks. The  $D^0$ ,  $D^+$ , and  $D^{*+}$   $R_{AA}$ , were measured for the first time as a function of transverse momentum and centrality. The suppression is almost as large as that observed for charged particles [ALICE 12g, Conesa del Valle 12] (see Fig. 17). A hint of non-zero flow of D hadrons was also measured [Ortona 12]. High precision measurements



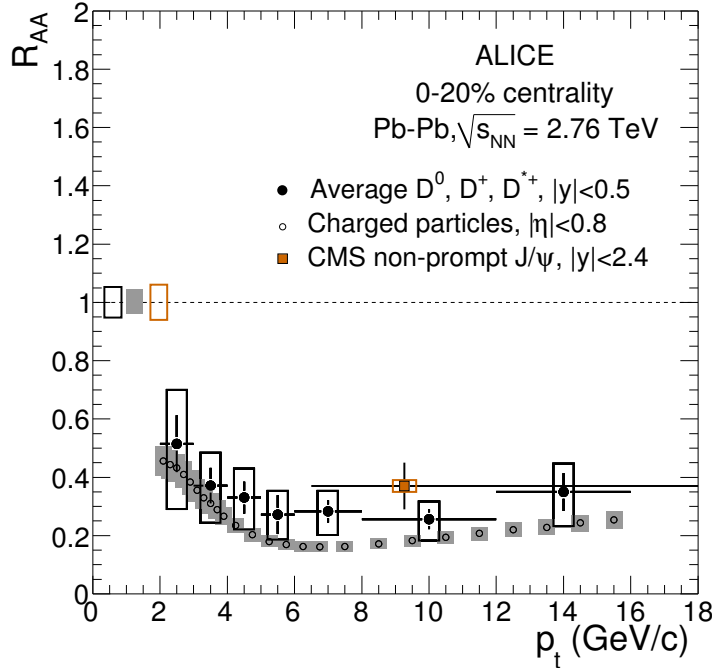


FIG. 17. Average  $R_{AA}$  of  $D$  mesons in the 0-20% centrality class compared to the nuclear modification factors of charged particles and non-prompt  $J/\psi$  from  $B$  decays measured by the CMS collaboration in the same centrality class. Figure 8 right in reference [ALICE 12g].

of heavy-flavour hadrons at low  $p_T$  will remain an experimental challenge during the next 10 years at RHIC and the LHC.

### E. The opacity of the QGP

Heavy ion collisions at LHC energies allowed to study for the first time the interaction between hard partons produced in the first stage of the hadronic collisions, with the QGP. The easiest experimental way to address this topic was via the study of high  $p_T$  particle yields and high  $p_T$  hadron-hadron correlations. High  $p_T$  particles are produced by the fragmentation of partons (quarks or gluons) in a time scale around  $\tau_{\text{frag}} \approx E/\Lambda_{\text{QCD}} \times R$ , where  $E$  is the energy of the parton and  $R$  is the typical size of a hadron ( $\sim 1$  fm). For energies above 5 GeV, the fragmentation time scale is about 20 fm/c. Therefore, in heavy ion collisions, partons are expected to fragment after traversing the QGP. One of the major discoveries at RHIC was the suppression of high  $p_T$  hadron  $R_{AA}$  and the quenching of back-to-back hadron correlations [STAR 02, PHENIX 03a, PHENIX 03b, BRAHMS 04, STAR 04a, PHENIX 05a]. This observation has been explained by the formation of a QGP drop where the initial hard partons interact losing a non negligible fraction of their initial energy (see section II F 3). QCD inspired models assuming gluon radiative energy loss in the QGP are in good agreement with the data [STAR 05b, PHENIX 05a]. On this topic the phenomenology is very rich and many experimental detailed studies have been performed [STAR 11b, STAR 12d, STAR 12b, PHENIX 08, PHENIX 12a].

The first LHC results on  $R_{AA}$  have confirmed RHIC results and extended the  $p_T$  ranges until values as high as 100 GeV/c [ALICE 11c, CMS 12e, ALICE 12a]. The results indicate a strong suppression of charged particle production in Pb-Pb collisions and a characteristic



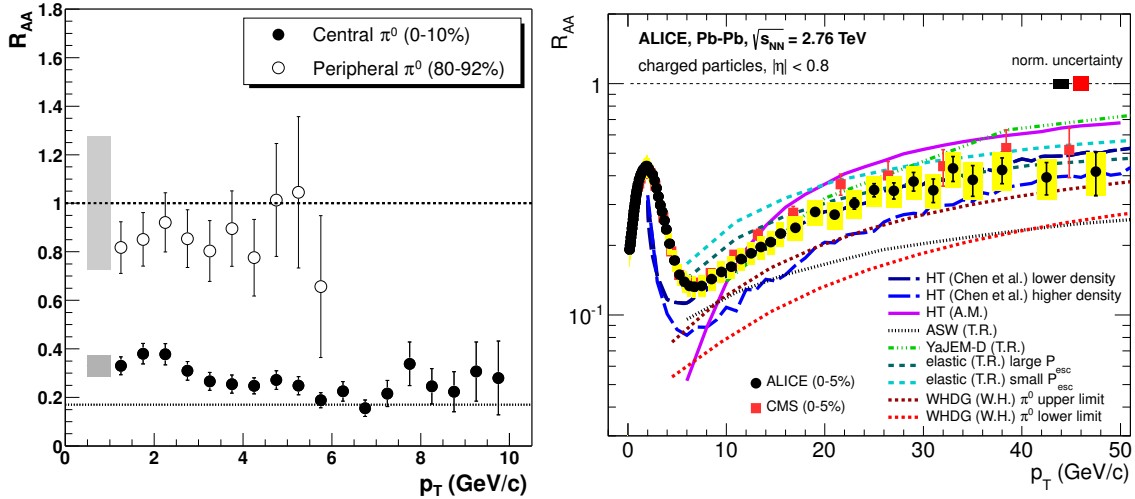


FIG. 18. *Left: Nuclear modification factor  $R_{AA}(p_T)$  for  $\pi^0$  in central (closed circles) and peripheral (open circles) Au-Au at  $\sqrt{s_{NN}} = 200$  GeV. Figure 3 from reference [PHENIX 03b]. Right:  $R_{AA}$  of charged particles measured by ALICE in the most central Pb-Pb collisions (0-5%) in comparison to results from CMS and model calculations. Figure 4 from reference [ALICE 12a]*

centrality and  $p_T$  dependence of the nuclear modification factors. In the most central collisions, the  $R_{AA}$  is strongly suppressed ( $R_{AA} \approx 0.13$ ) at  $p_T = 6-7$  GeV/c. Above  $p_T = 7$  GeV/c, there is a significant rise in the nuclear modification factor, which reaches  $R_{AA} \approx 0.4$  for  $p_T > 30$  GeV/c (see Fig. 18). The latter is in good agreement with models based on radiative energy loss of gluons in QGP.

At LHC the studies of jets in heavy ion collisions becomes possible. The ATLAS collaboration presented the first results on jet reconstruction in Pb-Pb collisions at the LHC [ATLAS 10]. Jets were reconstructed up to transverse energies of 100 GeV. An asymmetry, increasing with centrality, was observed between the transverse energies of the leading and second jets (see Fig. 19). This is an outstanding confirmation of the strong jet energy loss in a hot, dense medium, as it was inferred from the studies of the high  $p_T$   $R_{AA}$  and hadron correlations at RHIC. Similar conclusions were obtained from the measurement performed by the CMS collaboration [CMS 11b].

At LHC, the phenomenology on studies related to QCD energy loss is also very rich. Many measurements that are not described here have been performed, like hadron-hadron correlations [ALICE 12e], single jets [CMS 12h] and gamma-jets [CMS 12d]. In the next 10 years, high precision measurements will be performed on these channels and other more exotic ones, like Z-jet, will be studied.

The study of high  $p_T$   $R_{AA}$  of heavy flavour hadrons should shed light on the QCD energy loss mechanisms. According to QCD, the radiative energy loss of gluons should be larger than that of quarks. In addition, due to the dead cone effect [Dokshitzer 01], heavy quark energy loss should be further reduced with respect to that of light quarks. Many studies were performed at RHIC, mainly via the semileptonic decay of heavy flavour hadrons. A strong suppression was observed but quantitative conclusions are not yet available. At the LHC, ALICE collaboration has measured the high  $p_T$   $R_{AA}$  of  $D^0$ ,  $D^+$ , and  $D^{*+}$  [ALICE 12g, Conesa del Valle 12] and the high  $p_T$   $R_{AA}$  of semi-muonic decay of heavy-flavours (charm and beauty) [ALICE 12f]. The CMS collaboration has measured the high  $p_T$   $R_{AA}$  of  $J/\psi$  from beauty hadron decays. These results indicate strong in-medium energy loss for charm and beauty quarks, increasing towards the most central collisions. It seems that  $J/\psi$  from beauty hadron decays are less suppressed than charm hadrons, but systematic uncertainties are still large. In the next 10 years, thanks to the upgrades of the LHC and RHIC experiments,

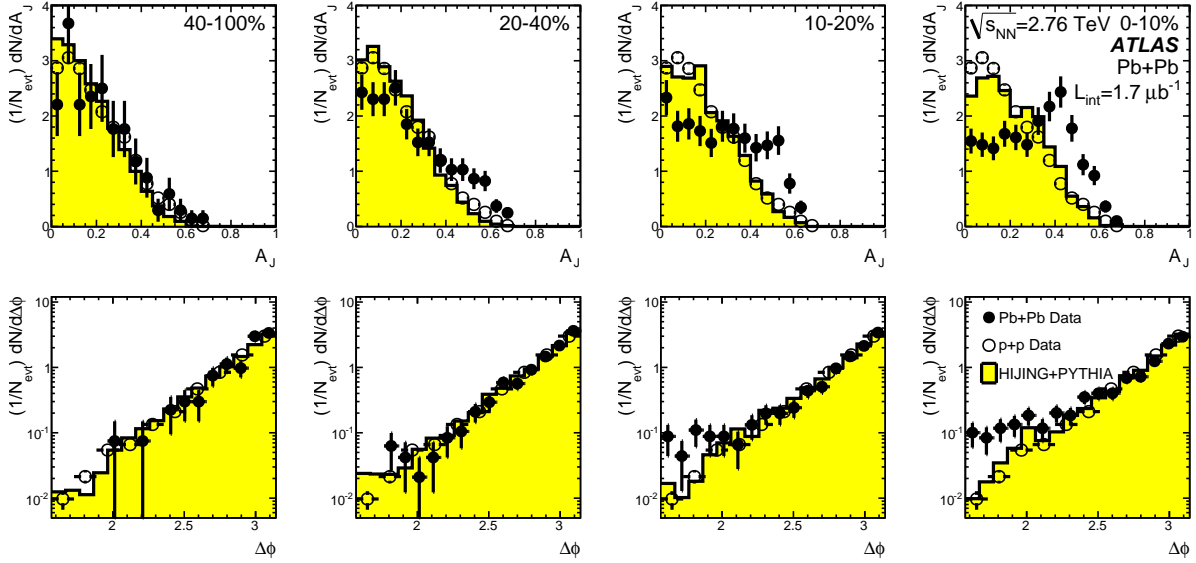


FIG. 19. *Top: dijet asymmetry distributions for data (points) and unquenched HIJING with superimposed PYTHIA dijets (solid yellow histograms), as a function of collision centrality (left to right from peripheral to central events). Proton-proton data from  $\sqrt{s} = 7$  TeV, analyzed with the same jet selection, is shown as open circles. Bottom: distribution of  $\Delta\phi$ , the azimuthal angle between the two jets, for data and HIJING+PYTHIA, also as a function of centrality. Figure 3 from reference [ATLAS 10].*

higher precision measurements will become available.

### F. Other interesting measurements

Among the huge amount of experimental results that have not been described in this section, I would like to quickly mention the following ones:

- The measurement of electro-weak boson  $R_{AA}$ , proposed by [Conesa del Valle 08], has become possible at LHC. CMS and ATLAS collaboration has performed the first measurements at the LHC [CMS 11c, ATLAS 12d, CMS 12f]. These have been fundamental measurements and (unfortunately) the measured nuclear modification factor is compatible with unity, as it was expected.
- The charged particle multiplicities measured in high-multiplicity pp collisions at LHC energies reach values that are of the same order as those measured in heavy-ion collisions at lower energies (e.g. they are well above the ones observed at RHIC for peripheral Cu-Cu collisions at 200 GeV [PHOBOS 11]). Therefore, it is a valid question whether pp collisions also exhibit any kind of collective behaviour as seen in these heavy-ion collisions. An indication for this might be the observation of long range, near-side angular correlations (ridge) in pp collisions at 0.9, 2.36 and 7 TeV with charged particle multiplicities above four times the mean multiplicity [CMS 10]. Recently  $J/\psi$  yields were measured for the first time in pp collisions as a function of the charged particle multiplicity density [ALICE 12c]. The study of high multiplicity pp and p-A collisions will be an exciting topic in the next years.
- Antimatter can efficiently be created in heavy ion collisions. STAR collaboration reported the first observation of the anti-helium-4 nucleus [STAR 11a].

- Finally, ultra-peripheral heavy ion collisions at RHIC and at the LHC have become a powerful high luminosity photon beam. Many interesting measurements of vector meson  $\rho$  [STAR 08, STAR 09b, STAR 11a], multi-pions [STAR 10b] or  $J/\psi$  [PHENIX 09a, ALICE 12b] are being performed in both colliders.

### G. Caveat on cold nuclear matter effects

This topic has not been addressed in the present proceedings. The study of cold nuclear matter effects in proton or deuteron induced collisions is of outstanding importance. Many of the interpretations of the experimental results given above can only be confirmed via the study of these collisions. At RHIC energies, deuteron induced collisions have been extensively studied. At LHC, the first run p-Pb has taken place beginning of 2013.

## VI. OTHER LECTURES ON QGP

The following references that will certainly complement the present lectures:

- Lectures of Larry MacLerran, *The Quark Gluon Plasma and The Color Glass Condensate: 4 Lectures* [Mc.Lerran 01].
- Lectures of Frithjof Karsch, *Lattice Results on QCD Thermodynamics* [Karsch 02a].
- Lectures of Jean-Paul Blaizot, *Theory of the Quark-Gluon Plasma* [Blaizot 02].
- Lectures of Ulrich W. Heinz, *Concepts of Heavy-Ion Physics* [Heinz 04].
- Lectures of Anton Andronic and Peter Braun-Munzinger, *Ultra relativistic nucleus-nucleus collisions and the quark-gluon plasma*, [Andronic 04].
- Lectures of Thomas Schaefer, *Phase of QCD* [Schaefer 05].
- Lectures of Bernt Müller, *From Quark-Gluon Plasma to the Perfect Liquid* [Müller 07].
- Lectures of Jean-Yves Ollitrault, *Relativistic hydrodynamics for heavy-ion collisions* [Ollitrault 07].
- Lectures of Tetsufumi Hirano, Naomi van der Kolk and Ante Bilandzic, *Hydrodynamics and Flow* [Hirano 08].
- Lectures of Carlos Salgado, *Lectures on high-energy heavy-ion collisions at the LHC* [Salgado 09].
- Article by Michael L. Miller, Klaus Reygers, Stephen J. Sanders, Peter Steinberg, *Glauber Modeling in High Energy Nuclear Collisions* [Miller 07].
- Article by David d'Enterria, *Hard scattering cross sections at LHC in the Glauber approach: from pp to pA and AA collisions* [d'Enterria 03].
- Article by Berndt Muller, Jurgen Schukraft and Bolek Wyslouch, *First Results from Pb+Pb collisions at the LHC* [Muller 12].
- In French: Proceedings of Joliot-Curie School in 1998: <http://www.cenbg.in2p3.fr/heberge/EcoleJoliotCurie/coursJC/JOLIOT-CURIE%201998.pdf> [Joliot-Curie 98].

- In French: Proceedings of Joliot-Curie School in 2005: <http://www.cenbg.in2p3.fr/heberge/EcoleJoliotCurie/coursJC/JOLIOT-CURIE%202005.pdf> [Joliot-Curie 05].
- In French: My HDR (Habilitation à Diriger des Recherches) [Martínez 06].

## VII. ACKNOWLEDGEMENTS

I would like to thank the organisers of the 2011 Joliot-Curie School for giving me the privilege to be one of the lecturers of this school which was devoted to the *Physics at the femtometer scale* and, namely, commemorated the 30th edition of the school.

I would like to thank Begoña de la Cruz, Hugues Delagrange, Javier Martin and Laure Massacrier for reading the manuscript, spotting many typos and making very interesting and fruitful comments.

I apologise to Navin Alahari, chairman of the Joliot Curie School, for the delay in getting ready these proceedings. He is the only person who knows how many electronic messages he sent to me as reminders of the different deadlines. Indeed he kindly agreed with several deadlines that I was not able to respect, except the last one.

- 
- [Abreu 08] S. Abreu & et al. *Heavy Ion Collisions at the LHC - Last Call for Predictions*. Journal of Physics G, page 054001, 2008. arXiv:0711.0974v1.
- [ALICE 10a] Collaboration ALICE. *Charged-particle multiplicity density at mid-rapidity in central Pb-Pb collisions at  $\sqrt{s_{NN}} = 2.76$  TeV*. Physical Review Letters, vol. 105, page 252301, 2010. arXiv:1011.3916.
- [ALICE 10b] Collaboration ALICE. *Elliptic flow of charged particles in Pb-Pb collisions at 2.76 TeV*. Physical Review Letters, vol. 105, page 252302, 2010. arXiv:1011.3914.
- [ALICE 11a] Collaboration ALICE. *Centrality dependence of the charged-particle multiplicity density at mid-rapidity in Pb-Pb collisions at  $\sqrt{s_{NN}} = 2.76$  TeV*. Physical Review Letters, vol. 106, page 032301, 2011. arXiv:1012.1657.
- [ALICE 11b] Collaboration ALICE. *Higher harmonic anisotropic flow measurements of charged particles in Pb-Pb collisions at  $\sqrt{s_{NN}} = 2.76$  TeV*. Physical Review Letters, vol. 107, page 032301, 2011. arXiv:1105.3865.
- [ALICE 11c] Collaboration ALICE. *Suppression of Charged Particle Production at Large Transverse Momentum in Central Pb-Pb Collisions at  $\sqrt{s_{NN}} = 2.76$  TeV*. Physics Letters B, vol. 696, pages 30–39, 2011. arXiv:1012.1004.
- [ALICE 12a] Collaboration ALICE. *Centrality Dependence of Charged Particle Production at Large Transverse Momentum in Pb-Pb Collisions at  $\sqrt{s_{NN}} = 2.76$  TeV*. Submitted to Physics Letters B, 2012. arXiv:1208.2711.
- [ALICE 12b] Collaboration ALICE. *Coherent  $J/\psi$  photoproduction in ultra-peripheral Pb-Pb collisions at  $\sqrt{s_{NN}} = 2.76$  TeV*. Submitted to Physics Letters B, 2012. arXiv:1209.3715.
- [ALICE 12c] Collaboration ALICE.  *$J/\psi$  Production as a Function of Charged Particle Multiplicity in pp Collisions at  $\sqrt{s} = 7$  TeV*. Physical Letters, vol. B712, pages 165–175, 2012.
- [ALICE 12d] Collaboration ALICE.  *$J/\psi$  suppression at forward rapidity in Pb-Pb collisions at  $\sqrt{s_{NN}} = 2.76$  TeV*. Physical Review Letters, vol. 109, page 072301, 2012. arXiv:1202.1383.
- [ALICE 12e] Collaboration ALICE. *Particle-yield modification in jet-like azimuthal di-hadron correlations in Pb-Pb collisions at  $\sqrt{s_{NN}} = 2.76$  TeV*. Physical Review Letters, vol. 108, page 092301, 2012. arXiv:1110.0121.
- [ALICE 12f] Collaboration ALICE. *Production of muons from heavy flavour decays at forward*

- rapidity in pp and Pb-Pb collisions at  $\sqrt{s_{NN}} = 2.76$  TeV.* Physical Review Letters, vol. 109, page 112301, 2012. arXiv:1205.6443.
- [ALICE 12g] Collaboration ALICE. *Suppression of high transverse momentum D mesons in central Pb-Pb collisions at  $\sqrt{s_{NN}} = 2.76$  TeV.* Journal of High Energy Physics, vol. 1209, page 112, 2012. arXiv:1203.2160.
- [Andronic 04] A. Andronic & P. Braun-Munzinger. *Ultrarelativistic nucleus-nucleus collisions and the quark-gluon plasma.* 2004. arXiv:hep-ph/0402291.
- [Andronic 09] A. Andronic, P. Braun-Munzinger & J. Stachel. *Thermal hadron production in relativistic nuclear collisions: the hadron mass spectrum, the horn, and the QCD phase transition.* Physics Letters B, vol. 673, page 142, 2009. arXiv:0812.1186.
- [Andronic 11] A. Andronic, P. Braun-Munzinger, K. Redlich & J. Stachel. *The thermal model on the verge of the ultimate test: particle production in Pb-Pb collisions at the LHC.* Proceedings of QM2011, 2011. arXiv:1106.6321v1.
- [Andronic 12] A. Andronic, P. Braun-Munzinger, K. Redlich & J. Stachel. *The statistical model in Pb-Pb collisions at the LHC.* 2012. arXiv:1210.7724.
- [Arleo 03] F. Arleo & et al. *CERN Yellow Report: Hard Probes in Heavy Ion Collisions at the LHC: Photon Physics.* 2003. hep-ph/0311131.
- [ATLAS 10] Collaboration ATLAS. *Observation of a Centrality-Dependent Dijet Asymmetry in Lead-Lead Collisions at  $\sqrt{s_{NN}} = 2.77$  TeV with the ATLAS Detector at the LHC.* Physical Review Letters, vol. 105, page 252303, 2010. arXiv:1011.6182.
- [ATLAS 12a] Collaboration ATLAS. *Measurement of the azimuthal anisotropy for charged particle production in  $\sqrt{s_{NN}} = 2.76$  TeV lead-lead collisions with the ATLAS detector.* Physical Review C, vol. 86, page 014907, 2012. arXiv:1203.3087.
- [ATLAS 12b] Collaboration ATLAS. *Measurement of the centrality dependence of the charged particle pseudorapidity distribution in lead-lead collisions at  $\sqrt{s_{NN}} = 2.76$  TeV with the ATLAS detector.* Physics Letters B, vol. 710, pages 363–382, 2012. arXiv:1108.6027.
- [ATLAS 12c] Collaboration ATLAS. *Measurement of the pseudorapidity and transverse momentum dependence of the elliptic flow of charged particles in lead-lead collisions at  $\sqrt{s_{NN}} = 2.76$  TeV with the ATLAS detector.* Physics Letters B, vol. 707, pages 330–348, 2012. arXiv:1108.6018.
- [ATLAS 12d] Collaboration ATLAS. *Measurement of Z boson Production in Pb+Pb Collisions at  $\sqrt{s_{NN}} = 2.76$  TeV with the ATLAS Detector.* 2012. arXiv:1210.6486.
- [Baier 97] R. Baier, Yu.L. Dokshitzer, A.H. Mueller, S. Peigné & D. Schiff. *Radiative energy loss of high energy quarks and gluons in a finite volume quark-gluon plasma.* Nuclear Physics B, vol. 483, 1997. arXiv:hep-ph/9607355.
- [Bedjidian 04] M. Bedjidian, D. Blaschke, Geoffrey T. Bodwin, N. Carrer, B. Cole et al. *Hard probes in heavy ion collisions at the LHC: Heavy flavor physics.* 2004. arXiv:hep-ph/0311048.
- [Beringer 12] J. Beringer et al. *Review of Particle Physics (RPP).* Physics Review D, vol. 86, page 010001, 2012. Web link to the PDG web site.
- [Bjorken 83] J.D. Bjorken. *Highly relativistic nucleus-nucleus collisions: The central rapidity region.* Physical Review D, vol. 27, page 140, 1983. Web link to this important paper.
- [Blaizot 99] J. P. Blaizot, Edmond Iancu & A. Rebhan. *Self-consistent hard-thermal-loop thermodynamics for the quark-gluon plasma.* Physics Letters B, vol. 470, page 181, 1999. arXiv:hep-ph/9910309.
- [Blaizot 02] Jean-Paul Blaizot. *Theory of the Quark-Gluon Plasma.* 2002. arXiv:hep-ph/0107131.
- [Bowick 85] M. J. Bowick & L. C. R. Wijewardhana. *Superstring at High Temperature.* Physical Review Letters, vol. 54, page 2485, 1985.
- [BRAHMS 04] Collaboration BRAHMS. *Evolution of the Nuclear Modification Factors with Rapidity and Centrality in d+Au Collisions at  $\sqrt{s_{NN}}=200$  GeV.* Physical Review Letters, vol. 93, page 242303, 2004. arXiv:nucl-ex/0403005.
- [BRAHMS 05] Collaboration BRAHMS. *Quark gluon plasma and color glass condensate at RHIC?*

- The perspective from the BRAHMS experiment.* Nuclear Physics A, vol. 757, page 1, 2005. arXiv:nucl-ex/0410020.
- [Braun-Munzinger 00] P. Braun-Munzinger & J. Stachel. *(Non)thermal aspects of charmonium production and a new look at  $J/\psi$  suppression.* Physics Letters B, vol. 490, page 196, 2000. arXiv:nucl-th/0007059.
- [Broniowski 04] Wojciech Broniowski, Wojciech Florkowski & Leonid Ya. Glozman. *Update of the Hagedorn mass spectrum.* Physical Review D, vol. 70, page 117503, 2004.
- [Cabibbo 75] N. Cabibbo & G. Parisi. *Exponential hadronic spectrum and quark liberation.* Physics Letters B, vol. 59, page 67, 1975.
- [CDF 88] Collaboration CDF. *Transverse-momentum distributions of charged particles produced in  $p - \bar{p}$  interactions at  $\sqrt{s}=630$  and  $1800$  GeV.* Physical Review Letters, vol. 61, page 1819, 1988.
- [CDF 90] Collaboration CDF. *Pseudorapidity distributions of charged particles produced in  $p$  anti- $p$  interactions at  $\sqrt{s}=630$  and  $1800$  GeV.* Physical Review D, vol. 41, page 2330, 1990.
- [CMS 10] Collaboration CMS. *Observation of Long-Range Near-Side Angular Correlations in Proton-Proton Collisions at the LHC.* JHEP, vol. 1009, page 091, 2010.
- [CMS 11a] Collaboration CMS. *Indications of suppression of excited  $\Upsilon$  states in PbPb collisions at  $\sqrt{s_{NN}} = 2.76$  TeV.* Physical Review Letters, vol. 107, page 052302, 2011. arXiv:1105.4894.
- [CMS 11b] Collaboration CMS. *Observation and studies of jet quenching in PbPb collisions at nucleon-nucleon center-of-mass energy  $= 2.76$  TeV.* Physical Review C, vol. 84, page 024906, 2011. arXiv:1102.1957.
- [CMS 11c] Collaboration CMS. *Study of Z boson production in PbPb collisions at nucleon-nucleon centre of mass energy of  $2.76$  TeV.* Physical Review Letters, vol. 106, page 212301, 2011. arXiv:1102.5435.
- [CMS 12a] Collaboration CMS. *Azimuthal anisotropy of charged particles at high transverse momenta in PbPb collisions at  $\sqrt{s[NN]} = 2.76$  TeV.* Physical Review Letters, vol. 109, page 022301, 2012. arXiv:1204.1850.
- [CMS 12b] Collaboration CMS. *Measurement of the pseudorapidity and centrality dependence of the transverse energy density in PbPb collisions at  $\sqrt{s[NN]} = 2.76$  TeV.* Physical Review Letters, vol. 109, page 152303, 2012. arXiv:1205.2488.
- [CMS 12c] Collaboration CMS. *Observation of sequential Upsilon suppression in PbPb collisions.* Accepted by Physical Review Letters, 2012. arXiv:1208.2826.
- [CMS 12d] Collaboration CMS. *Studies of jet quenching using isolated-photon+jet correlations in PbPb and pp collisions at  $\sqrt{s_{NN}} = 2.76$  TeV.* Accepted by Physics Letters B, 2012. arXiv:1205.0206.
- [CMS 12e] Collaboration CMS. *Study of high- $p_T$  charged particle suppression in PbPb compared to pp collisions at  $\sqrt{s_{NN}}=2.76$  TeV.* European Physics Journal, vol. C72, page 1945, 2012. arXiv:1202.2554.
- [CMS 12f] Collaboration CMS. *Study of W boson production in PbPb and pp collisions at  $\sqrt{s_{NN}} = 2.76$  TeV.* Physics Letters B, vol. 715, pages 66–87, 2012. arXiv:1205.6334.
- [CMS 12g] Collaboration CMS. *Suppression of non-prompt  $J/\psi$ , prompt  $J/\psi$ , and  $\Upsilon(1S)$  in PbPb collisions at  $\sqrt{s[NN]} = 2.76$  TeV.* Journal of High Energy Physics, vol. 1205, page 063, 2012. arXiv:1201.5069.
- [CMS 12h] Collaborations CMS. *Jet momentum dependence of jet quenching in PbPb collisions at  $\sqrt{s_{NN}}=2.76$  TeV.* Physics Letters B, vol. 712, pages 176–197, 2012. arXiv:1202.5022.
- [Collins 75] J.C. Collins & M.J. Perry. *Superdense Matter: Neutrons or Asymptotically Free Quarks?* Physical Review Letters, vol. 34, page 1353, 1975.
- [Conesa del Valle 08] Z. Conesa del Valle, A. Dainese, H.-T. Ding, G. Martinez Garcia & D.C. Zhou. *Effect of heavy-quark energy loss on the muon differential production cross-section in Pb-Pb collisions at  $\sqrt{s_{NN}} = 5.5$  TeV.* Physics Letters B, vol. 663, pages 202–208, 2008. arXiv:0712.0051.

- [Conesa del Valle 12] Z. Conesa del Valle. *D mesons suppression in PbPb collisions at  $\sqrt{s_{NN}} = 2.76$  TeV measured by ALICE*. 2012. Proceedings of Hard Probes 2012 arXiv:1210.2163.
- [d’Enterria 03] D. G. d’Enterria. *Hard scattering cross sections at LHC in the Glauber approach: from pp to pA and AA collisions*. 2003. arXiv:nucl-ex/0302016v3.
- [Dokshitzer 01] Yu. L. Dokshitzer & D. E. Kharzeev. *Heavy-quark colorimetry of QCD matter*. Physics Letters B, vol. 519, page 199, 2001.
- [Fodor 03] Zoltan Fodor. *Lattice QCD results at finite temperature and density*. Nuclear Physics A, vol. 715, page 319, 2003. arXiv:hep-lat/0209101.
- [Gelis 03] Francois Gelis. *QCD calculations of thermal photon and dilepton production*. Nuclear Physics A, vol. 715, page 329, 2003. arXiv:hep-ph/0209072.
- [Gelis 11] Francois Gelis. *Color Glass Condensate and Glasma*. Nuclear Physics A, vol. 854, pages 10–17, 2011. arXiv:1009.0093.
- [Gossiaux 09] P.B. Gossiaux, R. Bierkandt & J. Aichelin. *Tomography of a quark gluon plasma at RHIC and LHC energies*. Physical Review C, vol. 79, page 044906, 2009. arXiv:0901.0946.
- [Grandchamp 04] L. Grandchamp, R. Rapp & G.E. Brown. *In-Medium Effects on Charmonium Production in Heavy-Ion Collisions*. Physical Review Letters, vol. 92, page 212301, 2004.
- [Greiner 95] W. Greiner, L. Neise & H. Stoecker. *Thermodynamique et mécanique statistique*. Springer, 1995.
- [Griffiths 87] D. Griffiths. *Introduction to elementary particles*. Wiley, 1987.
- [Gross 73] D.J. Gross & F. Wilczek. *Ultraviolet Behavior of Non-Abelian Gauge Theories*. Physical Review Letters, vol. 30, page 1343, 1973.
- [Hagedorn 65] R. Hagedorn. *Statistical thermodynamics of strong interactions at high energies*. Nuovo Cimento Supplemento, vol. 3, page 147, 1965.
- [Hagedorn 84] R. Hagedorn. *Quark matter 84, proceedings helsinki*. Springer-Verlag, 1984. Contribution: How we got to QCD matter from the hadron side by trial and error.
- [Halzen 84] F. Halzen & A.D. Martin. *Quarks and leptons: An introductory course in modern particle physics*. John Wiley and Sons, 1984.
- [Heinz 04] Ulrich W. Heinz. *Concepts of Heavy-Ion Physics*. 2004. arXiv:hep-ph/0407360.
- [Hirano 08] Tetsufumi Hirano, Naomi van der Kolk & Ante Bilandzic. *Hydrodynamics and Flow*. 2008. arXiv:0808.2684.
- [Joliot-Curie 98] Ecole 1998 Joliot-Curie. *MATIERE HADRONIQUE : de la structure du nucléon au déconfinement des quarks*. 1998. Link to the proceedings.
- [Joliot-Curie 05] Ecole 2005 Joliot-Curie. *LA QCD A L’OEUVRE : des hadrons au plasma*. 2005. Link to the proceedings.
- [Karsch 02a] F. Karsch. *Lattice QCD at High Temperature and Density*. Lecture Notes of Physics, vol. 583, 2002. arXiv:hep-lat/0106019.
- [Karsch 02b] F. Karsch. *Lattice Results on QCD Thermodynamics*. Nuclear Physics A, vol. 698, 2002. arXiv:hep-ph/0103314.
- [Knecht 98] M. Knecht. *Une introduction la symétrie chirale*. École Joliot-Curie 1998, 1998. Link to the proceedings.
- [Landau 67] L. Landau & E. Lifchitz. *Physique statistique*. MIR, 1967.
- [Martínez 06] Ginés Martínez. *Introduction à l’étude expérimentale de la matière hadronique dans les collisions entre ions lourds. Le Plasma de Quarks et de Gluons*. 2006. Link to document in tel.archives-ouvertes.fr.
- [Massacrier 12] L. Massacrier.  *$J/\psi$  elliptic flow measurement in Pb-Pb collisions at  $\sqrt{s_{NN}} = 2.76$  TeV at forward rapidity with the ALICE experiment*. 2012. Proceedings of Hard Probes 2012, arXiv:1208.5401.
- [Matsui 86] T. Matsui & H. Satz.  *$J/\psi$  suppression by quark-gluon plasma formation*. Physics Letters B, vol. 178, page 416, 1986.
- [McLerran 01] L. McLerran. *The Color Glass Condensate and Small x Physics: 4 Lectures*. 2001. arXiv:hep-ph/0104285.

- [Miller 07] Michael L. Miller, Klaus Reygers, Stephen J. Sanders & Peter Steinberg. *Glauber Modeling in High Energy Nuclear Collisions*. 2007. arXiv:nucl-ex/0701025.
- [Müller 07] Berndt Müller. *From Quark-Gluon Plasma to the Perfect Liquid*. 2007. arXiv:0710.3366.
- [Muller 12] Berndt Muller, Jurgen Schukraft & Boleslaw Wyslouch. *First Results from Pb+Pb collisions at the LHC*. 2012. To appear in Annual Review of Nuclear and Particle Science. arXiv:1202.3233.
- [Nagle 10] J.L. Nagle, P. Steinberg & W.A. Zajc. *Quantitative and Conceptual Considerations for Extracting the Knudsen Number in Heavy Ion Collisions*. Physical Review C, vol. 81, page 024901, 2010. arXiv:0908.3684.
- [Ollitrault 93] Jean-Yves Ollitrault. *Determination of the reaction plane in ultrarelativistic nuclear collisions*. Physical Review D, vol. 48, pages 1132–1139, 1993. arXiv:hep-ph/9303247.
- [Ollitrault 07] Jean-Yves Ollitrault. *Relativistic hydrodynamics for heavy-ion collisions*. 2007. arXiv:0708.2433.
- [Ortona 12] Giacomo Ortona. *Open-charm meson elliptic flow measurement in Pb-Pb collisions at  $\sqrt{s_{NN}} = 2.76$  TeV with ALICE at the LHC*. 2012. Proceedings of Hard Probes 2012 arXiv:1207.7239.
- [Peigné 06] S. Peigné. *Chercheur CNRS de Subatech*. Private communication, 2006.
- [Petreczky 12] P. Petreczky. *Lattice QCD at non-zero temperature*. 2012. arXiv:1203.5320v1, Invited review for Journal of Physics G.
- [PHENIX 01] Collaboration PHENIX. *Measurement of the Midrapidity Transverse Energy Distribution from  $\sqrt{s_{NN}} = 130$  GeV Au-Au Collisions at RHIC*. Physical Review Letters, vol. 87, page 052301, 2001. arXiv:nucl-ex/0104015.
- [PHENIX 03a] Collaboration PHENIX. *Absence of Suppression in Particle Production at Large Transverse Momentum in  $\sqrt{s_{NN}} = 200$  GeV d+Au Collisions*. Physical Review Letters, vol. 91, page 072303, 2003. arXiv:nucl-ex/0306021.
- [PHENIX 03b] Collaboration PHENIX. *Suppressed  $\pi^0$  Production at Large Transverse Momentum in Central Au+Au Collisions at  $\sqrt{s_{NN}} = 200$  GeV*. Physical Review Letters, vol. 91, page 072301, 2003. arXiv:nucl-ex/0304022.
- [PHENIX 05a] Collaboration PHENIX. *Formation of dense partonic matter in relativistic nucleus-nucleus collisions at RHIC: Experimental evaluation by the PHENIX Collaboration*. Nuclear Physics A, vol. 757, page 184, 2005. arXiv:nucl-ex/0410003.
- [PHENIX 05b] Collaboration PHENIX. *Systematic studies of the centrality and  $\sqrt{s_{NN}} = 200$  GeV dependence of the  $dE_T/d\eta$  and  $dN_{ch}/d\eta$  in heavy ion collisions at midrapidity*. Physical Review C, vol. 71, 2005. arXiv:nucl-ex/0409015.
- [PHENIX 07] Collaboration PHENIX. *Centrality dependence of  $J/\psi$  production in Au + Au and Cu + Cu collisions by the PHENIX experiment at RHIC*. Journal of Physics G, vol. 34, pages S749–752, 2007. arXiv:nucl-ex/0703004.
- [PHENIX 08] Collaboration PHENIX. *Onset of  $\pi^0$  Suppression Studied in Cu+Cu Collisions at  $\sqrt{s_{NN}}=22.4, 62.4, \text{ and } 200$  GeV*. Physical Review Letters, vol. 101, page 162301, 2008. arXiv:0801.4555.
- [PHENIX 09a] Collaboration PHENIX. *Photoproduction of  $J/\psi$  and of high mass  $e^+e^-$  in ultra-peripheral Au+Au collisions at  $\sqrt{s_{NN}} = 200$ -GeV*. Physics Letters B, vol. 679, pages 321–329, 2009. arXiv:0903.2041.
- [PHENIX 09b] Collaboration PHENIX. *Systematic Studies of Elliptic Flow Measurements in Au+Au Collisions at  $\sqrt{s_{NN}} = 200$ -GeV*. Physical Review C, vol. 80, page 024909, 2009. arXiv:0905.1070.
- [PHENIX 10] Collaboration PHENIX. *Enhanced production of direct photons in Au+Au collisions at  $\sqrt{s_{NN}}=200$  GeV and implications for the initial temperature*. Physical Review Letters, vol. 104, page 132301, 2010. arXiv:0804.4168.
- [PHENIX 11a] Collaboration PHENIX. *Cold Nuclear Matter Effects on  $J/\psi$  Yields as a Func-*



- tion of Rapidity and Nuclear Geometry in Deuteron-Gold Collisions at  $\sqrt{s_{NN}} = 200$  GeV.* Physical Review Letters, vol. 107, page 142301, 2011. arXiv:1010.1246.
- [PHENIX 11b] Collaboration PHENIX. *J/ $\psi$  suppression at forward rapidity in Au+Au collisions at  $\sqrt{s_{NN}} = 200$  GeV.* Physical Review C, vol. 84, page 054912, 2011. arXiv:1103.6269.
- [PHENIX 12a] Collaboration PHENIX. *Evolution of  $\pi^0$  suppression in Au+Au collisions from  $\sqrt{s_{NN}} = 39$  to 200 GeV.* Physical Review Letters, vol. 109, page 152301, 2012. arXiv:1204.1526.
- [PHENIX 12b] Collaboration PHENIX. *J/ $\psi$  suppression at forward rapidity in Au+Au collisions at  $\sqrt{s_{NN}} = 39$  and 62.4 GeV.* 2012. arXiv:1208.2251.
- [PHOBOS 00] Collaboration PHOBOS. *Charged particle multiplicity near mid-rapidity in central Au+Au collisions at  $\sqrt{s} = 56$  and 130 AGeV.* Physical Review Letters, vol. 85, page 3100, 2000. arXiv:/hep-ex/0007036.
- [PHOBOS 02] Collaboration PHOBOS. *Energy dependence of particle multiplicities in central Au+Au collisions.* Physical Review Letters, vol. 88, page 022302, 2002. arXiv:nucl-ex/0108009.
- [PHOBOS 05] Collaboration PHOBOS. *The PHOBOS perspective on discoveries at RHIC.* Nuclear Physics A, vol. 757, page 28, 2005. arXiv:nucl-ex/0410022.
- [PHOBOS 06] Collaboration PHOBOS. *Energy dependence of directed flow over a wide range of pseudorapidity in Au+Au collisions at RHIC.* Physical Review Letters, page 012301, 2006. arXiv:nucl-ex/0511045.
- [PHOBOS 07] Collaboration PHOBOS. *System size, energy, pseudorapidity, and centrality dependence of elliptic flow.* Physical Review Letters, vol. 98, page 242302, 2007. arXiv:nucl-ex/0610037.
- [PHOBOS 11] Collaboration PHOBOS. *Phobos results on charged particle multiplicity and pseudorapidity distributions in Au+Au, Cu+Cu, d+Au, and p+p collisions at ultra-relativistic energies.* Physical Review C, vol. 83, page 024913, 2011. arXiv:1011.1940.
- [Politzer 73] H.D. Politzer. *Reliable Perturbative Results for Strong Interactions?* Physical Review Letters, vol. 30, page 1346, 1973.
- [Rajagopal 00] Krishna Rajagopal & Frank Wilczek. *The Condensed Matter Physics of QCD.* 2000. arXiv:hep-ph/0011333, At the Frontier of Particle Physics / Handbook of QCD III, Ed. M. Shifman (World Scientific).
- [Salgado 09] Carlos Salgado. *Lectures on high-energy heavy-ion collisions at the LHC.* The 2008 European School of High-Energy Physics, 2009. arXiv:0907.1219.
- [Schaefer 05] Thomas Schaefer. *Phases of QCD.* 2005. arXiv:hep-ph/0509068, Lectures at the Hampton University Graduate Studies Program (HUGS 2005).
- [Shuryak 78] Edward V. Shuryak. *Quark-Gluon Plasma and Hadronic Production of Leptons, Photons and Psions.* Physics Letters B, vol. 78, page 150, 1978.
- [Smilga 03] A. Smilga. *Professeur de l'Université de Nantes.* Private communication, 2003.
- [STAR 01] Collaboration STAR. *Elliptic flow in Au+Au collisions at  $\sqrt{s_{NN}} = 130$  GeV.* Physical Review Letters, vol. 86, page 402, 2001. arXiv-ex/0009011.
- [STAR 02] Collaboration STAR. *Disappearance of back-to-back high  $p_T$  hadron correlations in central Au + Au collisions at  $\sqrt{s_{NN}} = 200$  GeV.* Physical Review Letters, vol. 90, page 082302, 2002. arXiv:nucl-ex/0210033.
- [STAR 04a] Collaboration STAR. *Azimuthal anisotropy and correlations at large transverse momenta in p+p and Au+Au collisions at  $\sqrt{s_{NN}} = 200$  GeV.* Physical Review Letters, vol. 93, page 252301, 2004. arXiv:nucl-ex/0407007.
- [STAR 04b] Collaboration STAR. *Measurements of transverse energy distributions in Au+Au collisions at  $\sqrt{s_{NN}} = 200$  GeV.* Physical Review C, vol. 70, page 054907, 2004. arXiv:nucl-ex/0407003.
- [STAR 05a] Collaboration STAR. *Azimuthal Anisotropy in Au+Au Collisions at  $\sqrt{s_{NN}} = 200$  GeV.* Physical Review C, vol. 72, page 014904, 2005. arXiv:nucl-ex/0409033.

- [STAR 05b] Collaboration STAR. *Experimental and Theoretical Challenges in the Search for the Quark Gluon Plasma: The STAR Collaboration's Critical Assessment of the Evidence from RHIC Collisions*. Nuclear Physics A, vol. 757, page 102, 2005. arXiv:nucl-ex/0501009.
- [STAR 08] Collaboration STAR.  $\rho^0$  photoproduction in ultraperipheral relativistic heavy ion collisions. Physical Review C, vol. 77, page 034910, 2008. arXiv:0712.3320.
- [STAR 09a] Collaboration STAR.  $J/\psi$  production at high transverse momentum in  $p+p$  and  $Cu+Cu$  collisions at  $\sqrt{s_{NN}} = 200$  GeV. Physical Review C, vol. 80, page 041902, 2009. arXiv:0904.0439.
- [STAR 09b] Collaboration STAR. *Observation of two-source Interference in the Photoproduction Reaction  $Au+Au \Rightarrow Au+Au+\rho^0$* . Physical Review Letters, vol. 102, page 112301, 2009. arXiv:0812.1063.
- [STAR 10a] Collaboration STAR. *Identified particle production, azimuthal anisotropy, and interferometry measurements in  $Au+Au$  collisions at  $\sqrt{s_{NN}} = 9.2$  GeV*. Physical Review C, vol. 81, page 024911, 2010. arXiv:0909.4131.
- [STAR 10b] Collaboration STAR. *Observation of  $\pi^+\pi^-\pi^+\pi^-$  photoproduction in ultra-peripheral heavy ion collisions at STAR*. Physical Review C, vol. 81, page 044901, 2010. arXiv:0912.0604.
- [STAR 11a] Collaboration STAR. *Observation of the antimatter helium-4 nucleus*. Nature, vol. 473, page 353, 2011. arXiv:1103.3312.
- [STAR 11b] Collaboration STAR. *Studies of di-jet survival and surface emission bias in  $Au+Au$  collisions via angular correlations with respect to back-to-back leading hadrons*. Physical Review C, vol. 83, page 061901, 2011. arXiv:1102.2669.
- [STAR 12a] Collaboration STAR. *Directed and elliptic flow of charged particles in  $Cu+Cu$  collisions at  $\sqrt{s_{NN}} = 22.4$  GeV*. Physical Review C, vol. 85, page 014901, 2012. arXiv:1109.5446.
- [STAR 12b] Collaboration STAR. *Identified hadron compositions in  $p+p$  and  $Au+Au$  collisions at high transverse momenta at  $\sqrt{s_{NN}} = 200$  GeV*. Physical Review Letters, vol. 108, page 072302, 2012. arXiv:1110.0579.
- [STAR 12c] Collaboration STAR.  *$J/\psi$  production at high transverse momenta in  $p+p$  and  $Au+Au$  collisions at  $\sqrt{s_{NN}} = 200$  GeV*. 2012. arXiv:1208.2736.
- [STAR 12d] Collaboration STAR. *System size and energy dependence of near-side di-hadron correlations*. Physical Review C, vol. 85, page 014903, 2012. arXiv:1110.5800.
- [Stocker 99] H. Stocker, F. Jundt & G. Guillaume. *Toute la physique*. DUNOD, 1999.
- [Suire 12] Christophe Suire. *Charmonia production in ALICE*. 2012. Proceedings of Hard Probes 2012 arXiv:1208.5601.
- [Svetitsky 88] B. Svetitsky. *Diffusion of charmed quarks in the quark-gluon plasma*. Physical Review D, vol. 37, pages 2484–2491, 1988.
- [van Hees 08] H. van Hees, M. Mannarelli, V. Greco & R. Rapp. *Nonperturbative heavy-quark diffusion in the quark-gluon plasma*. Physical Review Letters, vol. 100, page 192301, 2008. <http://arxiv.org/abs/0709.2884> arXiv:0709.2884.
- [Wilczek 03] F. Wilczek. *Opportunities, Challenges, and Fantasies in Lattice QCD*. 2003. hep-lat/0212041 Keynote talk at Lattice 2002, Boston, June 2002.
- [Wilde 12] Martin Wilde. *Measurement of Direct Photons in  $pp$  and  $Pb-Pb$  Collisions with ALICE*. 2012. Proceedings of Quark Matter 2012 arXiv:1210.5958.
- [Zakharov 97] B.G. Zakharov. *Radiative energy loss of high-energy quarks in finite-size nuclear matter and quark-gluon plasma*. JETP Letter, vol. 65, 1997. arXiv:hep-ph/9704255.